GEOSPHERE

GEOSPHERE; v. 14, no. 3

https://doi.org/10.1130/GES01584.1

18 figures; 2 tables; 1 supplemental file

CORRESPONDENCE: pkempton@ksu.edu

CITATION: Kempton, P.D., Downes, H., and Lustrino, M., 2018, Pb and Hf isotope evidence for mantle enrichment processes and melt interactions in the lower crust and lithospheric mantle in Miocene orogenic volcanic rocks from Monte Arcuentu (Sardinia, Italy): Geosphere, v. 14, no. 3, https://doi.org/10.1130/GES01584.1.

Science Editor: Shanaka de Silva
Guest Associate Editor: Robert Stern
Associate Editor: Julie Roberge

Received 10 July 2017
Revision received 20 February 2018
Accepted 13 April 2018

Pb and Hf isotope evidence for mantle enrichment processes and melt interactions in the lower crust and lithospheric mantle in Miocene orogenic volcanic rocks from Monte Arcuentu (Sardinia, Italy)

Pamela D. Kempton[1], Hilary Downes[2], and Michele Lustrino[3,4]

[1]Department of Geology, Kansas State University, Manhattan, Kansas 66506, USA
[2]Department of Earth & Planetary Sciences, Birkbeck, University of London, WC1E 7HX, UK
[3]Dipartimento di Scienze della Terra, Università degli Studi di Roma La Sapienza, P.le A. Moro, 5, 00185 Roma, Italy
[4]Istituto di Geologia Ambientale e Geoingegneria (IGAG) - CNR, c/o Dipartimento di Scienze della Terra, Università degli Studi di Roma La Sapienza, P.le A. Moro, 5, 00185 Roma, Italy

ABSTRACT

Miocene (ca. 18 Ma) subduction-related basalts and basaltic andesites from Monte Arcuentu, southern Sardinia, Italy, show a remarkable correlation between $^{87}Sr/^{86}Sr$ (from ~0.705 to ~0.711) over a small range of SiO_2 (~51–58 wt%) that contrasts with most other orogenic volcanic suites worldwide. New high-precision Pb and Hf isotope data help to constrain the petrogenesis of these rocks.

The most primitive Monte Arcuentu rocks (MgO >8.5 wt%) were sourced from a mantle wedge metasomatized by melts derived from terrigenous sediment, likely derived from Archean terranes of northern Africa. This gave rise to magmas with high $^{87}Sr/^{86}Sr$ (0.705–0.709) and $^{207}Pb/^{204}Pb$ (15.65–15.67) with moderate εHf (–1 to +8) and εNd (–6 to +1), but it does not account for the full range of compositions observed. More evolved rocks (MgO <8.5 wt%) have higher $^{87}Sr/^{86}Sr$ (up to 0.711) and $^{207}Pb/^{204}Pb$ (up to 15.68), with εHf and εNd as low as –8 and –9, respectively. Mixing calculations suggest that evolved rocks with low Rb/Ba and low $^{206}Pb/^{204}Pb$ interacted with lower crust similar compositionally to that exposed today in Calabria, Italy, which was formerly in crustal continuity with Sardinia. High Rb/Ba and high $^{206}Pb/^{204}Pb$ magmas interacted with lithospheric mantle similar to that sampled by Italian lamproites. Partial melting of lower crustal and upper mantle lithologies was facilitated by the rapid extension, and subsequent passive mantle upwelling, that occurred as Sardinia drifted away from the European plate during the Oligo-Miocene (ca. 32–15 Ma). Fractional crystallization under these PT conditions involved olivine + clinopyroxene with little or no plagioclase, such that differentiation proceeded without significant increase in SiO_2. The Monte Arcuentu rocks provide insights into assimilation process in the lower crust and lithospheric mantle that may be obscured by upper crustal assimilation–fractional crystallization (AFC) processes in other orogenic suites.

INTRODUCTION

Establishing the geochemical characteristics of the mantle beneath the western Mediterranean, and the processes that gave rise to those characteristics, is essential for understanding the geodynamic evolution of the region (Peccerillo and Lustrino, 2005; Avanzinelli et al., 2009; Lustrino et al., 2011). However, the range of petrologic components and processes that may be involved, particularly in subduction-related magma genesis, makes this a challenging task.

High-field-strength elements (HSFE) are commonly used to investigate subduction petrogenesis, because they tend to behave in a "conservative" fashion, i.e., immobile and retained in the subducted slab (Pearce et al., 1995; Keppler, 2017; Zirakparvar, 2017). Thus, they may provide the best chance to identify a geochemical "baseline" from which to estimate fluxes of more mobile elements (Pearce et al., 2007). It is argued that Hf isotopes can also be used to "see through" subduction processes into the nature of the sub-arc mantle wedge (Kempton et al., 2001; Jicha et al., 2004; Barry et al., 2006; Pearce et al., 2007). In contrast, mobile or "non-conservative" elements, such as large-ion-lithophile elements (LILE), are readily mobilized by fluids and easily transported from the slab into the mantle wedge. Volcanic arc magmas derived by melting of that mantle are then enriched in those elements.

However, Hf may not always behave as a conservative element, particularly where partial melting of subducted sediments is involved (Woodhead et al., 2001; Hanyu et al., 2002; Münker et al., 2004; Tollstrup and Gill, 2005; Tollstrup et al., 2010; Handley et al., 2011). Therefore, where sub-arc mantle enrichment processes are dominated by aqueous fluids, Hf is likely to be conservative, but where silicate melts are involved, particularly of subducted sediments, Hf may behave in a non-conservative fashion.

Here we examine a suite of subduction-related rocks from Monte Arcuentu, Sardinia, Italy, in the western Mediterranean, not only to better understand the

geodynamic evolution of this region, but also to further explore the behavior of Hf during subduction and the question of sediment melt versus aqueous fluid enrichment of the mantle wedge. We have chosen this locality because previous research has suggested the petrogenesis of these rocks was dominated by mantle metasomatic processes rather than crustal contamination (Downes et al., 2001). Here we report new Hf and high-precision Pb isotope data for the previously studied samples.

The Cenozoic igneous rocks of Sardinia can be divided into two main groups (Lustrino et al., 2011, 2013): a late Eocene–middle Miocene subduction-related (SR; ca. 38–15 Ma) group and a middle Miocene–Pleistocene anorogenic group (ca. 12–0.1 Ma). Our study focuses on the Monte Arcuentu volcano products belonging to the older activity. We will show that Monte Arcuentu is geochemically distinct from the rest of the SR magmatism on Sardinia, and other orogenic magmatism globally, preserving a record of its metasomatized mantle source in the most primitive rocks, which is overprinted by interaction with lithospheric mantle and/or lower crust in the more evolved rocks.

GEOLOGIC BACKGROUND

Sardinia, Italy, and Corsica, France, form a small continental micro-plate in the western Mediterranean, situated between Neogene oceanic-type crust and thinned continental crust of the Tyrrhenian Sea to the east and the Ligurian-Provençal Basin to the west (Fig. 1). It consists of an ~25–35-km-thick crust (Splendore and Marotta, 2013), whose late Precambrian to Paleozoic basement was deformed and metamorphosed during the Caledonian and Hercynian orogenies and extensively intruded by calc-alkaline granitoids (Tommasini et al., 1995; Rossi et al., 2009; Casini et al., 2015). The basement is overlain by Mesozoic sediments that were deposited when Sardinia was part of the passive margin of southern Europe (Carminati et al., 2010).

The geodynamics of the western Mediterranean are complex, but essentially involve subduction with different polarities of the Alpine Tethys oceanic lithosphere due to northward migration of Africa during the Mesozoic (Réhault et al., 1984, 2012; Carminati et al., 2010). Detailed reviews of the geologic evolution of the region are given by Carminati et al. (2012), Lustrino et al. (2013) and references therein, so only essential aspects will be mentioned here.

During the Cretaceous, subduction was oriented in a southeast direction beneath the approaching African promontory known as Adria, but once it had docked with Europe during the Eocene, the direction of subduction of Tethys lithosphere flipped and the remaining oceanic lithosphere was subducted west-northwest beneath Europe, giving birth to the Apennine-Maghrebian subduction system (Fig. 1B; Gueguen et al.; 1998; Carminati et al., 2012; Lustrino et al., 2017). At the beginning of the Oligocene, Sardinia was part of the Iberian Peninsula, but back-arc spreading split it away, initiating a southeast-directed drifting stage from ca. 32–23 Ma. The Sardinia–Corsica micro-plate then began rotating ~60° counterclockwise during the Miocene (23–15 Ma) until it reached its current position and orientation during the Langhian (Gattacceca et al., 2007; Advokaat et al., 2014) (Fig. 1B). During middle to late Miocene, oceanic slab roll-back resulted in passive asthenospheric upwelling in the back-arc domain and opening of the Ligurian-Provençal Basin (Lustrino et al., 2009). At ca. 10 Ma, back-arc basin spreading resumed east of Sardinia–Corsica, eventually leading to formation of the Tyrrhenian Sea (Carminati et al., 2010, 2012). The subduction hinge also shifted eastward, where it exists today beneath Calabria and the Aeolian arc.

The late Eocene–middle Miocene SR volcanism on Sardinia consists of medium-K arc tholeiites to high-K calc-alkaline rocks, mostly emplaced during an Aquitanian-Langhian flare-up phase (Beccaluva et al., 1985; Lecca et al., 1997; Morra et al., 1997; Lustrino et al., 2009; Conte et al., 2010). The earliest sporadic volcanic products (ca. 38–24 Ma) were andesitic, whereas the bulk of the magmatism (22 and 18 Ma) consisted of dacite to rhyolite ignimbrite flows (e.g., Lecca et al., 1997) associated with formation of the Sardinia Rift (Fig. 1). Minor products were generated until ca. 15 Ma in the southern (e.g., Sulcis; Morra et al., 1994; Conte et al., 2010; Gisbert and Gimeno, 2017) and central sectors of the island (e.g., Mt. Arci). With relocation of the subduction zone farther east—roughly coeval with the opening of the Tyrrhenian Sea and the potassic-ultrapotassic volcanism of peninsular Italy—the late Miocene to Pleistocene (ca. 12–0.1 Ma) volcanism of Sardinia shifted abruptly from orogenic to anorogenic in character, with sodic alkaline to tholeiitic lavas (Lustrino et al., 2007; 2013).

Our study builds on that of Downes et al. (2001) of the Miocene Monte Arcuentu volcano, located within the southern extension of the Oligo–Miocene Sardinia Rift on the southern margin of the younger (Plio–Pleistocene) Campidano graben (Fig. 1A). Earlier studies encompassed a wider geographic area, referred to collectively as the Arcuentu Volcanic Complex (Assorgia et al., 1995; Brotzu et al., 1997). These studies include a more compositionally diverse volcano-sedimentary succession that has been divided into four units (A to D) based on age (Brotzu et al., 1997). The eruptive products include a thick set of lavas (unit C; ca. 20–18 Ma) that overlie older submarine volcaniclastic deposits (units A and B; ca. 30–22 Ma). The volcaniclastic deposits are crosscut by numerous, ca. 18-m.y.-old basaltic dikes (unit D; ca. 18–17 Ma). The samples for our study are from the uppermost (Burdigalian age) units located at the center of the complex at Monte Arcuentu, equivalent to upper unit C and unit D of Brotzu et al. (1997).

GEOCHEMISTRY OF THE ARCUENTU ROCKS

Arcuentu volcanic rocks (here including both Arcuentu Volcanic Complex and Monte Arcuentu) are largely basaltic andesites with minor basalts and andesites (Downes et al., 2001; Franciosi et al., 2003; Lustrino et al., 2013). They are distinct from most other SR volcanic rocks of Sardinia in that they have lower total alkalis ($Na_2O + K_2O$) for a given SiO_2, and highly evolved compositions are absent (Fig. 2). In an AFM diagram (Fig. 3), the Arcuentu rocks straddle the boundary between tholeiitic and calc-alkaline rocks proposed by Irvine and Baragar (1971), but a traditional Peacock (1931) plot clearly classifies them as calcic rather than calc-alkaline (Fig. 4). Figure 3 also shows that their high MgO character places them among the most primitive of Sardinia SR rocks.

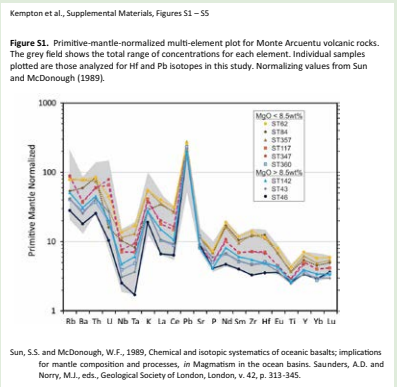

[1]Supplemental Figures. S1: Primitive-mantle-normalized multi-element plot for Monte Arcuentu volcanic rocks. S2: SiO_2 versus selected major and trace elements from Monte Arcuentu and other Sardinia subduction-related (SR) rocks. S3: SiO_2 versus selected major and trace elements from Monte Arcuentu and other Sardinia SR rocks. S4: SiO_2 versus selected major and trace elements from Monte Arcuentu and other Sardinia SR rocks. S5: Selected major and trace elements versus MgO for Monte Arcuentu and other Sardinia SR rocks. Please visit https://doi.org/10.1130/GES01584.S1 or the full-text article on www.gsapubs.org to view the Supplemental Figures.

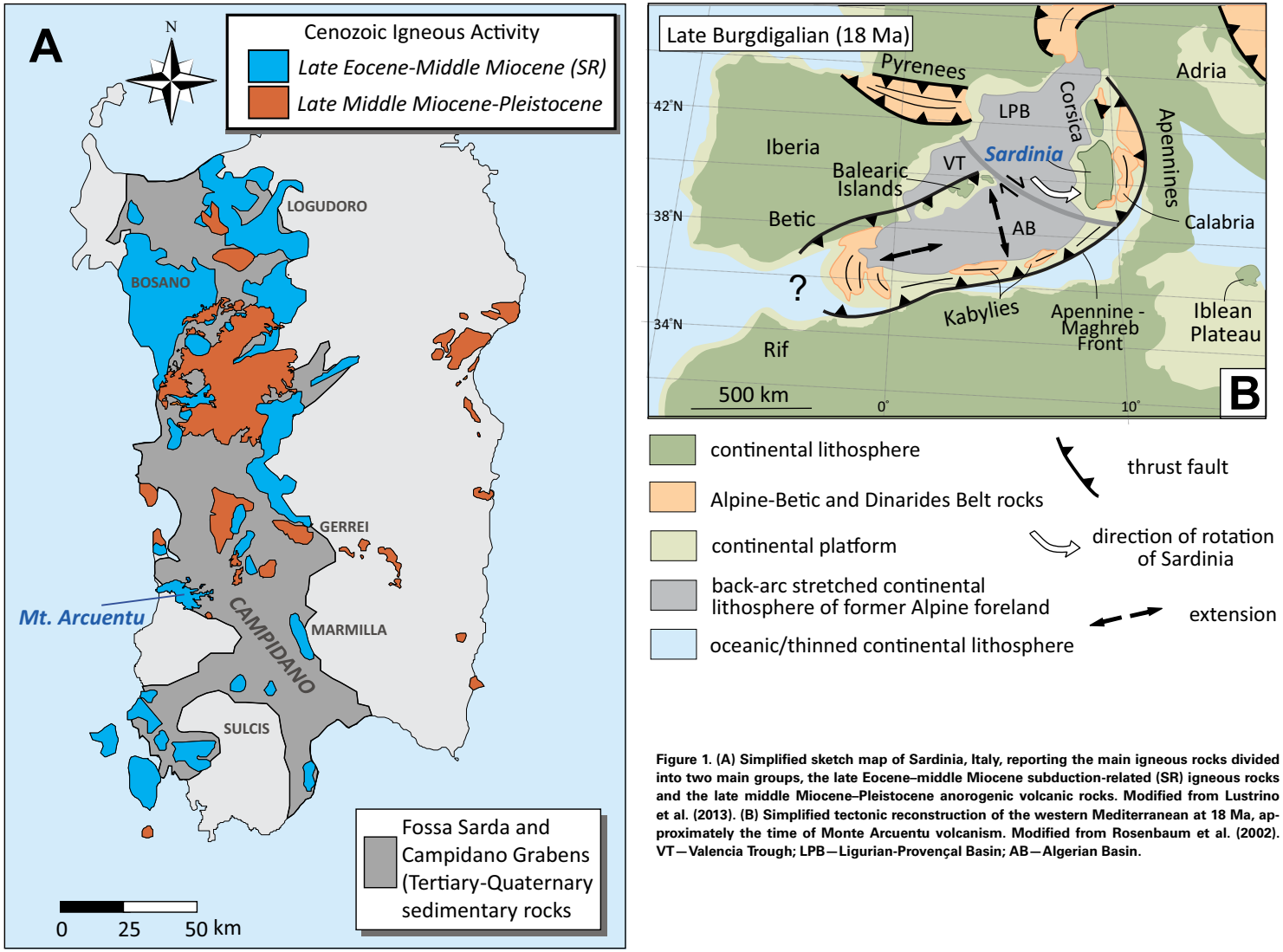

Figure 1. (A) Simplified sketch map of Sardinia, Italy, reporting the main igneous rocks divided into two main groups, the late Eocene–middle Miocene subduction-related (SR) igneous rocks and the late middle Miocene–Pleistocene anorogenic volcanic rocks. Modified from Lustrino et al. (2013). (B) Simplified tectonic reconstruction of the western Mediterranean at 18 Ma, approximately the time of Monte Arcuentu volcanism. Modified from Rosenbaum et al. (2002). VT—Valencia Trough; LPB—Ligurian-Provençal Basin; AB—Algerian Basin.

Major and trace element variations versus MgO (Downes et al., 2001) highlight the dominant role of mafic mineral fractionation in producing much of the observed compositional spectrum.

Arcuentu rocks have trace element features typical of other SR magmas worldwide, i.e., strong depletions in the HFSE such as Nb, Ta, and Ti; enrichment in LILE such as Rb, Ba, and Th; high concentrations of Pb and enrichment of light rare-earth elements (LREE) relative to heavy rare-earth elements (HREE) (Supplemental Fig. S1[1]). However, there are noticeable differences between Arcuentu rocks and other Sardinia SR rocks in the abundances and evolutionary trends of several key major and trace elements (Fig. 5). Other SR rocks show decreasing TiO_2 with increasing SiO_2, whereas Arcuentu shows only a weak correlation between these two elements and, if anything, the

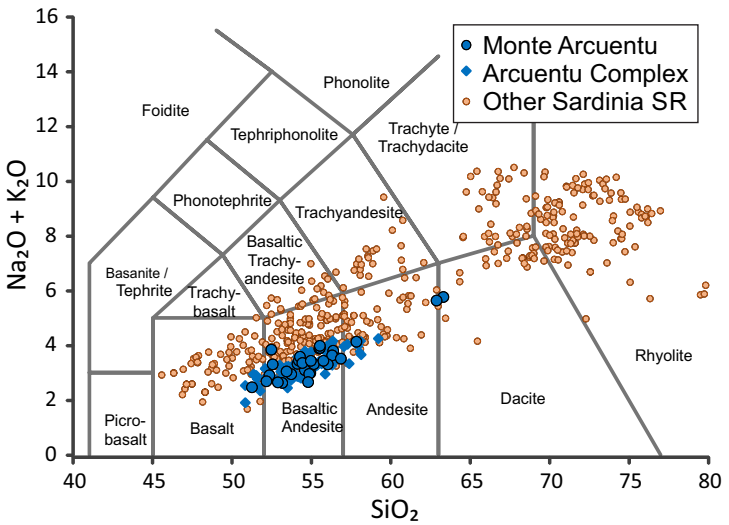

Figure 2. Total Alkalis versus SiO_2 classification diagram (Le Maitre et al., 2002) for Monte Arcuentu volcanic rocks compared with other Sardinia SR rocks. Data from compilation of Lustrino et al. (2013); references available therein.

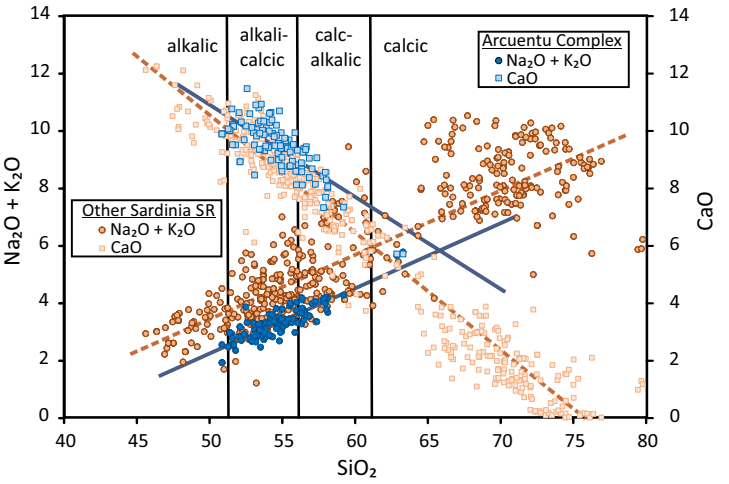

Figure 4. Traditional Peacock (1931) plot of $Na_2O + K_2O$ and CaO vs SiO_2. The intersection points of the respective regression lines indicate that Arcuentu rocks (blue symbols) are classified as calcic, whereas other Sardinia SR rocks (brown symbols) are borderline calc-alkalic. Data sources as in Figure 2.

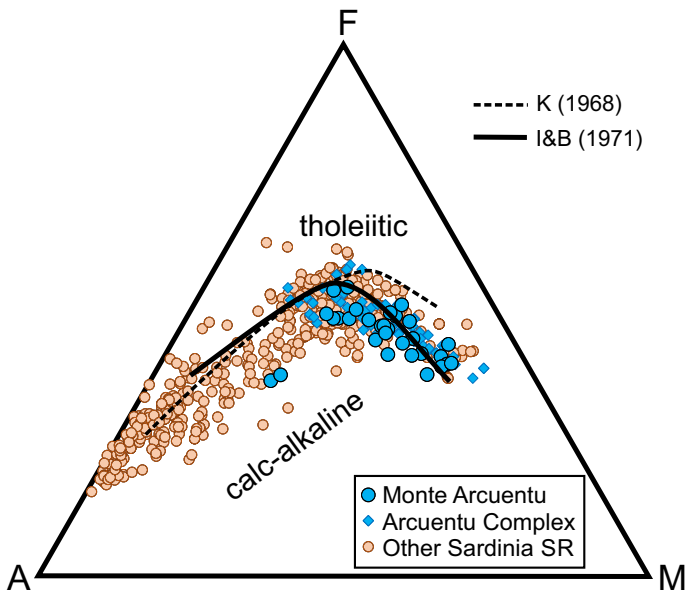

Figure 3. AFM (total alkalis, FeO_{tot}, MgO) diagram with boundary curves between calc-alkaline and tholeiitic from Kuno (1968) (K), and Irvine and Baragar (1971) (I&B).

opposite trend. Furthermore, concentrations of TiO_2 and Al_2O_3 (Figs. 5A and 5B), as well as P_2O_5 (Fig. S2A [footnote 1]), tend to be lower for a given SiO_2 content than in other Sardinia SR rocks. Both Arcuentu and other Sardinia SR rocks exhibit weak negative correlations between CaO/Al_2O_3 versus SiO_2 and Mg# [i.e., Mg/(Mg+(0.9*Fe))] versus SiO_2, but the trends for Arcuentu rocks are much steeper and the values higher, on average, for a given SiO_2 (Figs. S2B and S2C). Their relatively primitive nature is demonstrated by their Ni (Fig. 5C) and Cr (Fig. S2D) contents. Conversely, Sr concentrations are significantly lower for a given SiO_2 than other Sardinia SR rocks (Fig. 5D).

Compositional similarities between the Arcuentu rocks and some other Sardinia SR rocks are noteworthy. Some rocks from Montresta and Marmilla, Sardinia, Italy, have high MgO, Ni, and Cr contents, but most of these rocks have lower SiO_2 contents (Morra et al., 1997; Mattioli et al., 2000); they are also isotopically distinct (discussed below).

RESULTS

Our new Hf and high-precision Pb isotope data for Monte Arcuentu are presented in Table 1 and Figures 6–8, where they are shown relative to other Cenozoic volcanic rocks of the western Mediterranean. Analytical details can be found in the Appendix. In the $^{176}Hf/^{177}Hf$ versus $^{143}Nd/^{144}Nd$ diagram (Fig. 6), Monte Arcuentu rocks form an array that plots roughly parallel to the Terrestrial Array (Vervoort et al., 2011), with εHf values ranging from +8 to –8 and ΔεHf (i.e., the vertical deviation from the terrestrial array) ranging from –0.2

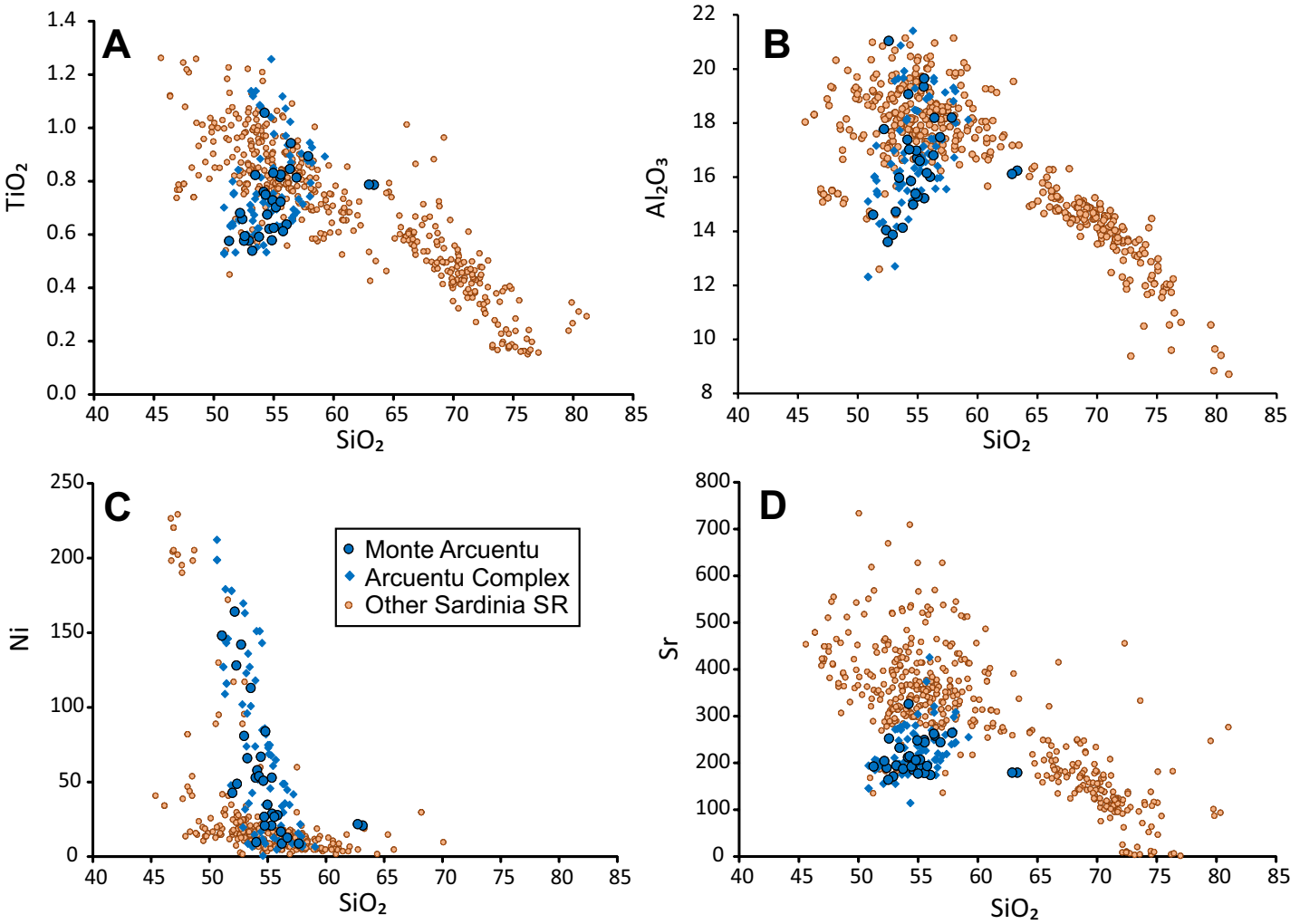

Figure 5. Selected major and trace elements versus SiO_2 for Monte Arcuentu and other Sardinia SR rocks. Data sources as in Figure 2. TiO_2 values for six samples from Marmilla, Italy, are known to be in error (Mattioli, pers. comm.) and have been excluded from the diagram.

to +3.7. The most radiogenic compositions are only slightly less radiogenic than calc-alkaline volcanics from the Aeolian islands of Alicudi and Filicudi. Peccerillo et al. (1993) interpreted these islands as being derived from mantle sources that are among the least modified by subduction zone processes in the Aeolian arc. In contrast, the least radiogenic Hf and Nd isotope compositions overlap the fields for Roman Province volcanics and Italian lamproites. Hercynian lower crustal xenoliths and sediments from the Eastern Mediterranean and Ionian Sea exhibit wide ranges in Nd and Hf isotope values and overlap the Monte Arcuentu rocks for all but the most radiogenic compositions. There are few published Hf isotope data for other Sardinia SR rocks, but the three samples reported by Lustrino et al. (2013) plot parallel to and slightly below the Monte Arcuentu array, close to the Terrestrial Array (Fig. 6).

TABLE 1. Hf AND Pb ISOTOPE DATA FOR MONTE ARCUENTU BASALTS AND BASALTIC ANDESITES

Sample		Lu	Hf	$^{176}Hf/^{177}Hf$	εHf_{18}	$^{206}Pb/^{204}Pb$	$^{207}Pb/^{204}Pb$	$^{208}Pb/^{204}Pb$
ST43	Dike	0.22	1.5	0.282795	0.95	18.6177	15.6651	38.7824
ST46	Dike	0.27	1.1	0.283010	8.40	18.6758	15.6441	38.7187
ST62	Lava	0.44	3.6	0.282557	–7.41	18.5745	15.6778	38.9546
ST84	Breccia	0.37	3.9	0.282572	–6.84	18.5806	15.6833	39.0440
ST117	Lava	0.31	2.2	0.282702	–2.33	18.7421	15.6822	38.7447
ST142	Dike	0.25	1.5	0.282754	–0.53	18.6899	15.6725	38.9102
ST347	Lava		2.1	0.282671	–3.42*	18.7627	15.6812	38.7644
ST357	Lava	0.40	3.5	0.282568	–6.81	18.5894	15.6815	38.9263
ST360	Lava	0.26	1.6	0.282909	4.95	18.6619	15.6565	38.7865

Notes: Age data from Assorgia et al. (1995). Lu and Hf concentrations from Downes et al. (2001).
*Lu concentration not available; εHf calculated assuming an average $^{176}Lu/^{177}Hf$ for the suite of 0.021.

In a $^{207}Pb/^{204}Pb$ versus $^{206}Pb/^{204}Pb$ diagram (Fig. 7A), the Monte Arcuentu data plot between the HIMU (i.e., high μ, where $\mu = {}^{238}U/{}^{204}Pb$) and EM (enriched mantle) end-members of Stracke (2012). They have high $^{207}Pb/^{204}Pb$ values for a given $^{206}Pb/^{204}Pb$, in common with most volcanic rocks from the Aeolian arc and central Italy. Monte Arcuentu rocks have lower $^{206}Pb/^{204}Pb$ than most other orogenic magmatism of the region but show some overlap with rocks from the Roman Province and Italian lamproites (Figs. 7A and 7B). They exhibit a Y-shaped vertical array, the low $^{207}Pb/^{204}Pb$ end of which points toward the composition of some tholeiitic basalts from the Tyrrhenian Sea (Fig. 7A). The high $^{207}Pb/^{204}Pb$–high $^{206}Pb/^{204}Pb$ branch overlaps the compositions of Eastern Mediterranean sediments, as well as Italian lamproites, although most of the sediments have higher $^{206}Pb/^{204}Pb$ and $^{207}Pb/^{204}Pb$. The high $^{207}Pb/^{204}Pb$–low $^{206}Pb/^{204}Pb$ branch extends toward the compositions of some Hercynian basement rocks of Calabria and lower crustal xenoliths from the Massif Central. In contrast, most other Sardinia SR rocks have lower $^{207}Pb/^{204}Pb$ and/or $^{206}Pb/^{204}Pb$ ratios (Fig. 7B) that scatter between the Campanian Province field and unradiogenic Plio–Pleistocene anorogenic volcanics (UPV) of Sardinia (Fig. 7).

Many of the older literature data in this diagram appear to exhibit vertical arrays similar to Monte Arcuentu. However, most of these older data were collected using thermal ionization mass spectrometry, the analytical uncertainty for which is usually an order of magnitude greater or more than that of the new multicollector–inductively coupled plasma–mass spectrometer (MC-ICP-MS) Pb data reported here for Monte Arcuentu. Because the variations in $^{207}Pb/^{204}Pb$ tend to be small, this greater analytical uncertainty can make it difficult to recognize trends within these older data.

In $^{208}Pb/^{204}Pb$ versus $^{206}Pb/^{204}Pb$ space, the Monte Arcuentu rocks plot at a steep angle to the trends exhibited by most localities of the western Mediterranean (Fig. 8A), clearly indicating that mixing is responsible for the Pb isotope variations. The low $^{208}Pb/^{204}Pb$ end of the array trends toward Tyrrhenian Sea tholeiites, overlapping the fields for Eastern Mediterranean and Ionian Sea sediments, whereas the high $^{208}Pb/^{204}Pb$ data trend toward the compositions of some Calabrian basement and Hercynian lower crust (Fig. 8B), although these crustal rocks exhibit a considerable range in Pb isotope compositions.

DISCUSSION

Crustal Contamination versus Source Enrichment

Based on major and trace element modeling, Brotzu et al. (1997) concluded that the petrogenesis of Arcuentu Complex rocks was dominated by fractional crystallization in mid- to shallow crustal reservoirs and that crustal contamination was negligible. Focusing on the rocks from Monte Arcuentu, as opposed to the broader Arcuentu complex, Downes et al. (2001) reinforced this conclusion using Sr, Nd, and O isotope data, and instead attributed the observed isotopic variations to mantle metasomatism, i.e., enrichment of the sub-arc mantle wedge via subduction. One aspect of the geochemistry that strongly supports this argument is the unusual variation shown by the Monte Arcuentu rocks in $^{87}Sr/^{86}Sr$ versus SiO_2 (Fig. 9). In this diagram, the Monte Arcuentu samples display a remarkably steep correlation that contrasts with most other orogenic volcanic rocks. Arc volcanics from Tonga-Fiji-Vanuatu and the Northern, Central, and Southern Volcanic Zones of the Andes, for example, exhibit broad trends with slopes that are much shallower than the Arcuentu Complex (Fig. 9A). Rocks from the Altiplano-Puna back-arc region of the Central Andes exhibit greater compositional diversity, but the increase in $^{87}Sr/^{86}Sr$ with increasing SiO_2 for individual centers is still significantly less than that observed for the Arcuentu Complex (Fig. 9A; see Figs. S3A–S3C [footnote 1]). At low SiO_2 contents, subduction enrichment is likely to be responsible for at least some of the increase in $^{87}Sr/^{86}Sr$ relative to depleted mantle, but the spread to high SiO_2 is generally ascribed to combined fractional crystallization—assimilation in crustal magma chambers and/or deep crustal MASH (Melting, Assimilation, Stagnation, Homogenization; Hildreth and Moorbath, 1988) zones. Data for several islands of the Aeolian Arc follow similar trends to those of the Andes and Tonga-Fiji-Vanuatu. Rocks from Alicudi have low, depleted-mantle-like $^{87}Sr/^{86}Sr$ and hence record the smallest degree of subduction enrichment among Aeolian arc volcanoes (Peccerillo et al., 1993). The horizontal arrays for Vulcano and Stromboli, with their higher $^{87}Sr/^{86}Sr$ compositions, indicate either progressively greater mantle enrichment or crustal contamination (or

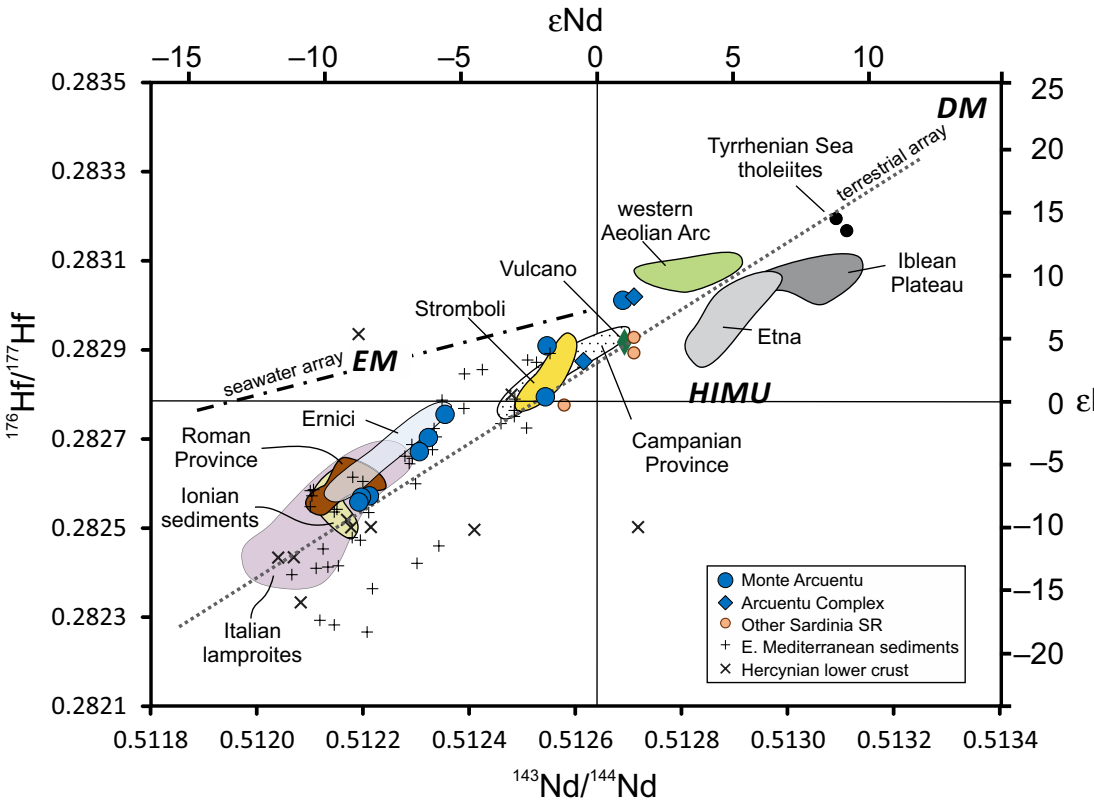

Figure 6. εHf versus εNd showing rocks for Monte Arcuentu relative to other volcanic rocks of the western Mediterranean. Data sources for this and subsequent isotope diagrams are listed in Table A1. Enriched mantle (EM), depleted mantle (DM), and high μ (HIMU) components from Stracke (2012). Terrestrial Array from Vervoort et al. (2011). Seawater Array from Albarède et al. (1998).

both). In contrast, the steep array for Monte Arcuentu overlaps the fields for medium- to high-K volcanics of central-southern Italy (Campanian Province, Ernici-Roccamonfina, Vulsini Mountains) and trends toward the field for Italian lamproites. Although the Monte Arcuentu rocks are clearly not as K-rich as the Italian lamproites, the trend suggests that metasomatized mantle, similar to that producing the potassic and ultrapotassic magmas of central Italy, was involved in their petrogenesis.

The Monte Arcuentu rocks also contrast with the other Sardinia SR rocks (Fig. 9B). Instead of the steep, well-defined trend shown by Monte Arcuentu, other SR rocks form a broad, concave downward array that extends both to lower and higher SiO_2, but with a more limited range in $^{87}Sr/^{86}Sr$. None of the other Sardinia SR rocks have $^{87}Sr/^{86}Sr$ values greater than ~0.709, whereas the Monte Arcuentu rocks have $^{87}Sr/^{86}Sr$ values up to ~0.711. Conversely, the lowest $^{87}Sr/^{86}Sr$ for Monte Arcuentu is ~0.705, even for basaltic rocks with relatively high Mg numbers [i.e., Mg# >0.68], whereas ~10% of the other SR rocks have $^{87}Sr/^{86}Sr$ less than ~0.705, some as low as 0.7035 (Lustrino et al., 2013).

Within the broad array of Sardinia SR rocks, each volcanic center tends to be slightly different, so the data are summarized in Figure 9C using a best-fit polynomial to represent each center. For most centers, the curves show an overall positive correlation between $^{87}Sr/^{86}Sr$ and SiO_2, suggesting that the magmas have undergone moderate amounts of crustal contamination (Lustrino et al., 2013). However, two areas show an unusual pattern in which the $^{87}Sr/^{86}Sr$ values decrease as the magmas become more evolved. This has been interpreted by Lustrino et al. (2013) as evidence that the most differentiated SR rocks formed by partial melting of preexisting basaltic lower crust. The downward limb of the curve represents a mixing trajectory between mildly evolved and contaminated melts of the upward limb (i.e., $^{87}Sr/^{86}Sr$ increasing with SiO_2) and silica-rich partial melts derived from previously underplated basaltic/gabbroic SR rocks. This model requires an exceptional heat source to produce siliceous melts from mafic lower crust, which Lustrino et al. (2013) argue was due to rapid upwelling of hot asthenospheric mantle resulting from high rates of separation of Sardinia from continental Europe during the Oligo–Miocene (Morra et al., 1997; Mattioli et al., 2000).

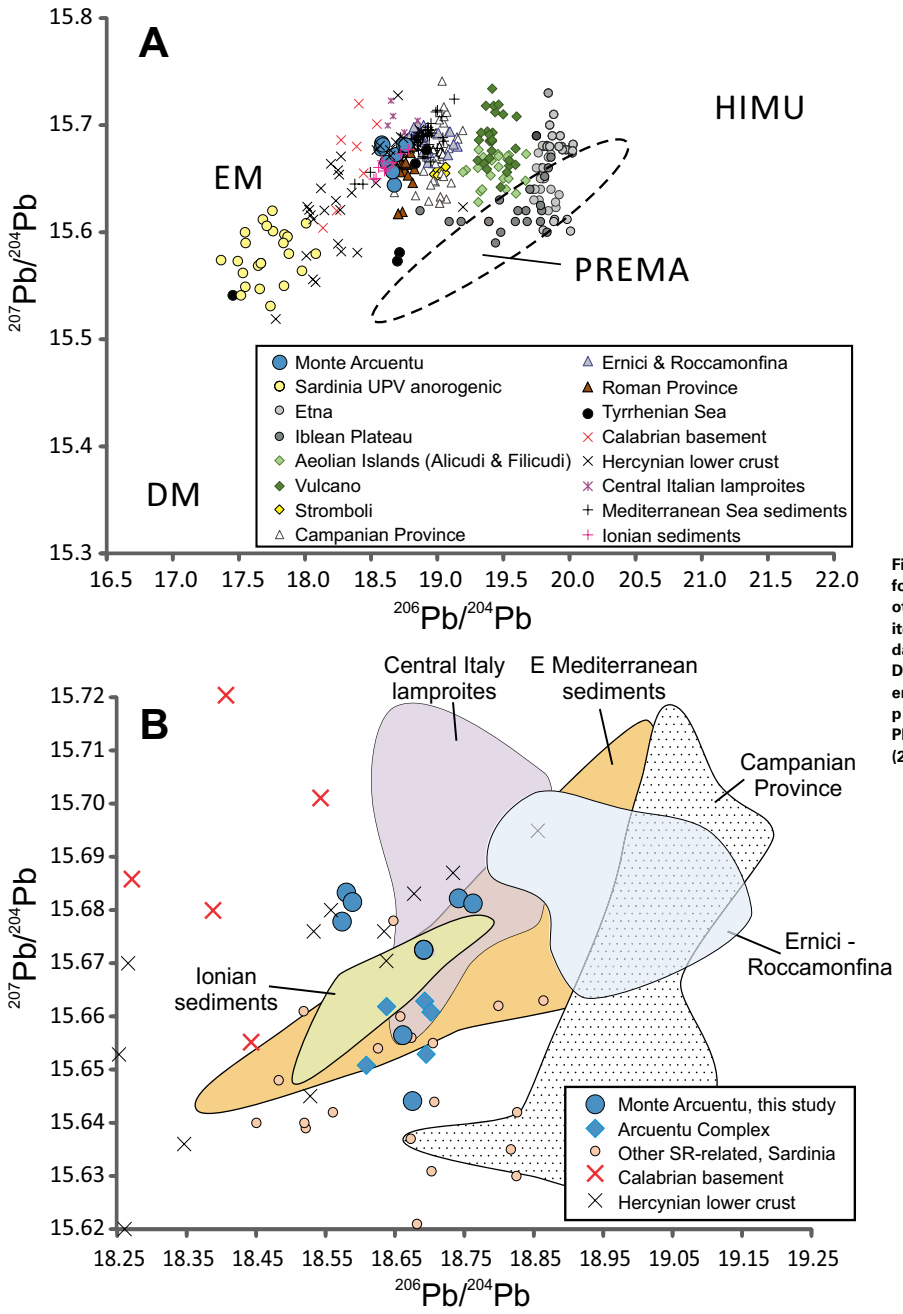

Figure 7. (A) $^{207}Pb/^{204}Pb$ versus $^{206}Pb/^{204}Pb$ for Monte Arcuentu rocks relative to other volcanic rocks of the western Mediterranean. (B) Detail of Monte Arcuentu data relative to other Sardinia SR rocks. Data sources listed in Table A1. Mantle end-members (HIMU—high μ; DM—depleted mantle; EM—enriched mantle; PREMA—prevalent mantle) from Stracke (2012). UPV—unradiogenic Pb volcanics.

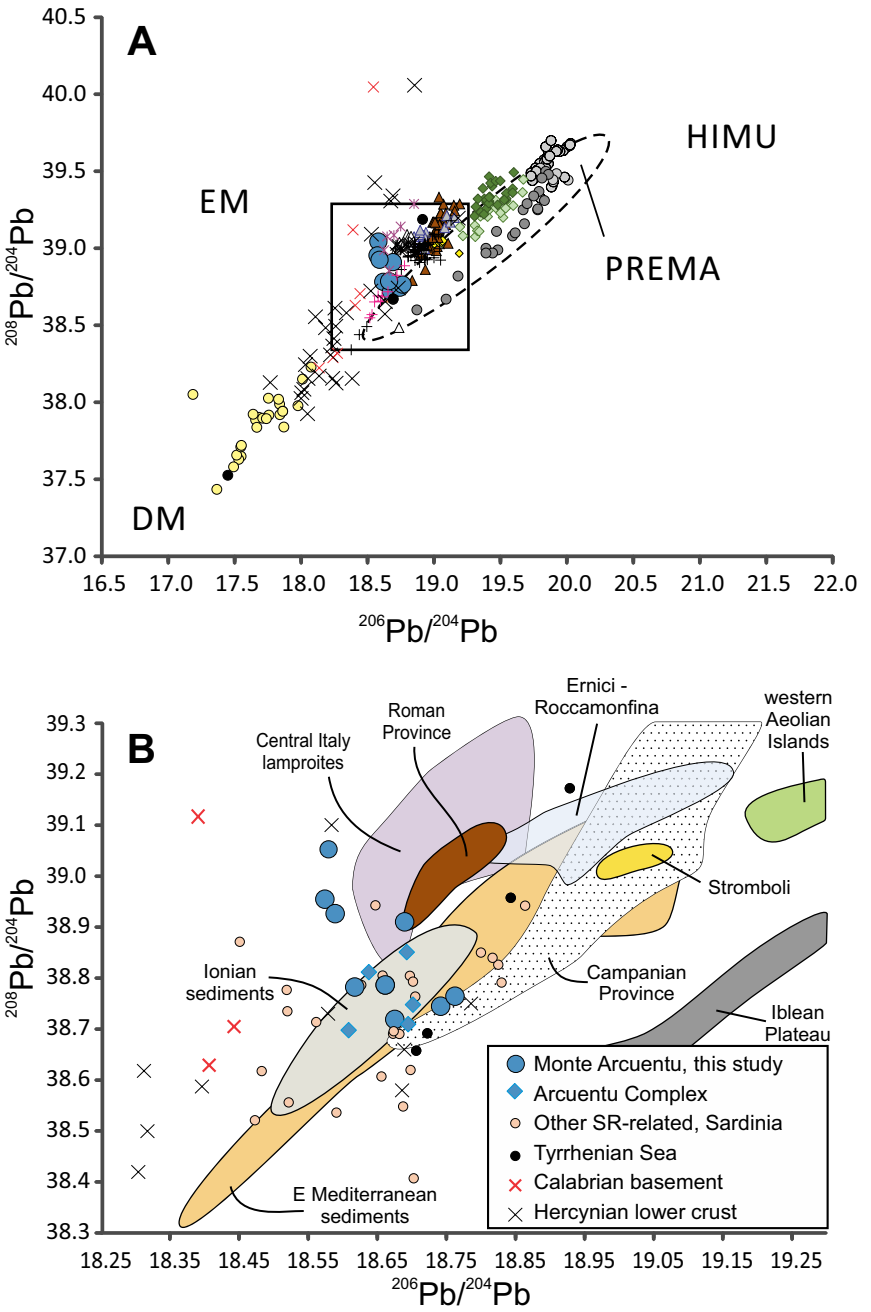

Figure 8. (A) $^{208}Pb/^{204}Pb$ versus $^{206}Pb/^{204}Pb$ for Monte Arcuentu rocks relative to other volcanic rocks of the western Mediterranean. Symbols as in Figure 7A. (B) Detail of Monte Arcuentu data relative to other SR rocks of Sardinia. Data sources listed in Table A1. Mantle end-members are as defined in Figure 7.

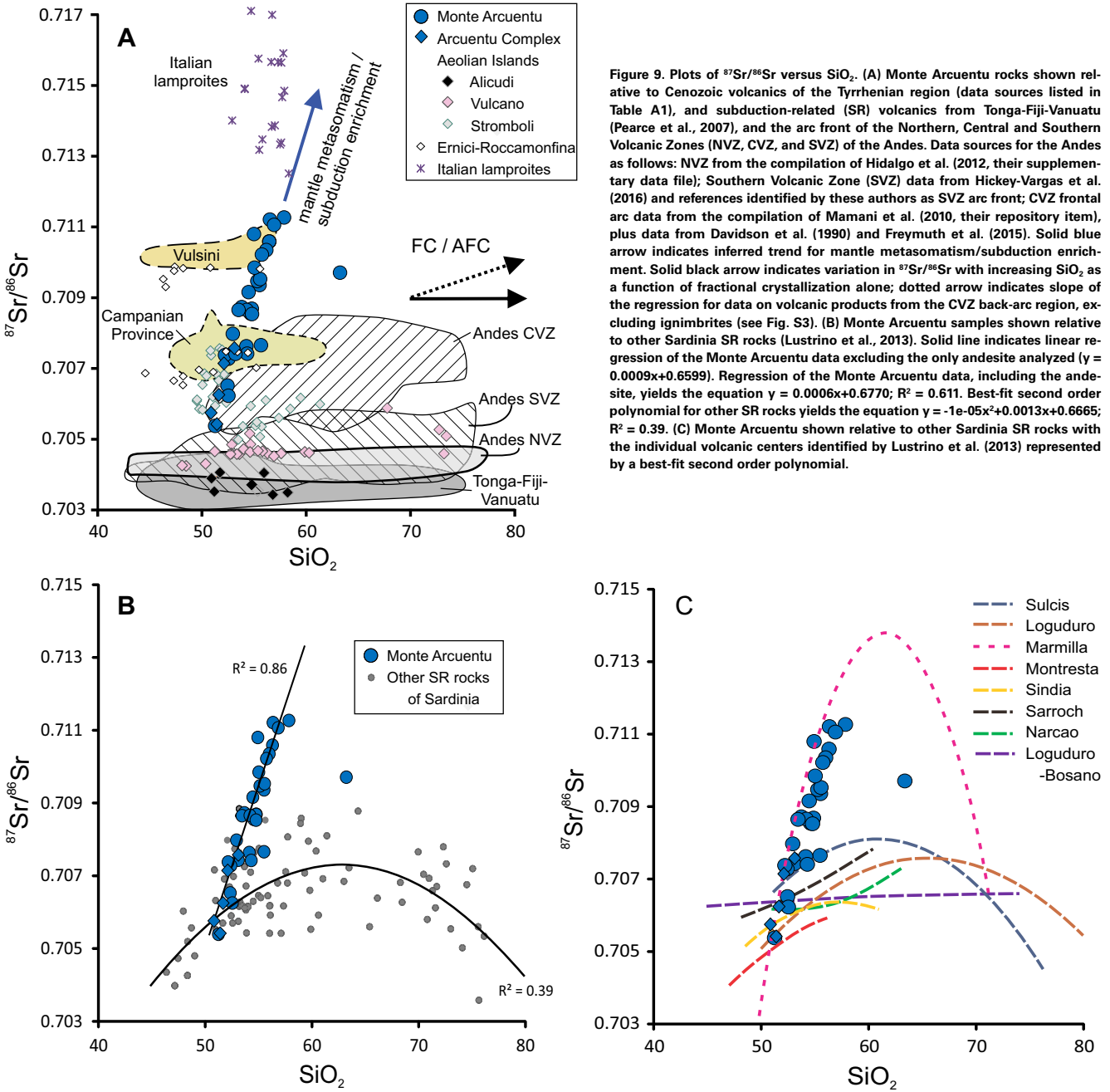

Figure 9. Plots of $^{87}Sr/^{86}Sr$ versus SiO_2. (A) Monte Arcuentu rocks shown relative to Cenozoic volcanics of the Tyrrhenian region (data sources listed in Table A1), and subduction-related (SR) volcanics from Tonga-Fiji-Vanuatu (Pearce et al., 2007), and the arc front of the Northern, Central and Southern Volcanic Zones (NVZ, CVZ, and SVZ) of the Andes. Data sources for the Andes as follows: NVZ from the compilation of Hidalgo et al. (2012, their supplementary data file); Southern Volcanic Zone (SVZ) data from Hickey-Vargas et al. (2016) and references identified by these authors as SVZ arc front; CVZ frontal arc data from the compilation of Mamani et al. (2010, their repository item), plus data from Davidson et al. (1990) and Freymuth et al. (2015). Solid blue arrow indicates inferred trend for mantle metasomatism/subduction enrichment. Solid black arrow indicates variation in $^{87}Sr/^{86}Sr$ with increasing SiO_2 as a function of fractional crystallization alone; dotted arrow indicates slope of the regression for data on volcanic products from the CVZ back-arc region, excluding ignimbrites (see Fig. S3). (B) Monte Arcuentu samples shown relative to other Sardinia SR rocks (Lustrino et al., 2013). Solid line indicates linear regression of the Monte Arcuentu data excluding the only andesite analyzed (y = 0.0009x+0.6599). Regression of the Monte Arcuentu data, including the andesite, yields the equation y = 0.0006x+0.6770; R^2 = 0.611. Best-fit second order polynomial for other SR rocks yields the equation y = -1e-05x^2+0.0013x+0.6665; R^2 = 0.39. (C) Monte Arcuentu shown relative to other Sardinia SR rocks with the individual volcanic centers identified by Lustrino et al. (2013) represented by a best-fit second order polynomial.

The best fit curve through the data for Marmilla forms a steep parabola that passes through most of the Monte Arcuentu data. However, all but one sample from Marmilla plot within the low SiO_2 end of the Monte Arcuentu array ($^{87}Sr/^{86}Sr$ <0.7088); therefore, the parabola is constrained by one evolved sample only (with ~71 wt% SiO_2). Nonetheless, the Marmilla samples show some major and trace element similarities to the Monte Arcuentu rocks, e.g., low Al_2O_3 and high MgO for a given SiO_2. These two localities are separated by less than 30 km across the Campidano graben and prior to this Plio–Pleistocene extension would have been even closer, suggesting they may record similar petrogenetic processes.

A second argument presented by Downes et al. (2001) in favor of subduction-modified mantle sources for Monte Arcuentu magmas is the variation of Sr isotopes with $\delta^{18}O$. In $\delta^{18}O$ versus $^{87}Sr/^{86}Sr$ (not shown), the data for clinopyroxene separates form a positive correlation that is only slightly concave upward (Downes et al., 2001). Calculated mixing curves between primitive Monte Arcuentu basalts and Hercynian felsic granulites pass through the majority of the data but require assimilation in excess of 40% felsic crust. Assimilation of this much felsic crust by the most primitive basaltic rocks in the suite would result in significant increases in SiO_2, which are not observed.

Source Enrichment

Sediment Melting versus Fluid Fluxing

If we accept that crustal contamination is not the main process responsible for the compositional variations observed within the Monte Arcuentu suite, then the likely alternative is source enrichment. Melting of a pyroxenite-rich sub-arc mantle (e.g., Lambart et al., 2013) can be ruled out on the basis of major and trace element systematics (see Figs. S4A and S4B [footnote 1]). We, therefore, consider source enrichment via sediments recycled during subduction, as suggested by the $^{87}Sr/^{86}Sr$ versus SiO_2 trend (Fig. 9A). The questions that follow are: (a) What was the nature of the sediments? and, (b) Was the process controlled by dehydration of sediments or was sediment melting involved?

Numerous studies have now shown that Hf, and to a lesser extent Nd, tend to behave as conservative elements in the arc environment when aqueous fluids alone are involved (Johnson and Plank, 1999; Kempton et al., 2001; Barry et al., 2006; Pearce et al. 2007). Assuming a mantle source similar to that for Etna as the composition of the unmodified mantle wedge (Fig. 6), the Monte Arcuentu samples with the most depleted Nd and Hf isotopic ratios could be explained by interaction between that mantle and fluids derived from subducted sediments. That is, subduction fluxing by aqueous fluid carrying Nd (as a non-conservative element) but little Hf (a conservative element) could reduce the Nd isotope ratio of the mantle wedge while having little effect on the Hf isotope composition (Pearce et al., 2007). The result would be an offset in isotopic composition like that observed between Etna and the most depleted Monte Arcuentu rocks (Fig. 6). However, this mechanism by itself cannot account for the more enriched isotope signatures observed within the Monte Arcuentu suite. It is also inconsistent with the Pb isotope systematics (Fig. 7), since Monte Arcuentu samples do not plot along a mixing line between sediments and Etna mantle. Therefore, sediment melting is required to explain the full range of εNd and εHf values for Monte Arcuentu rocks.

Trace element plots, such as Th/Nb versus Ba/Nb (Fig. 10), also support an origin via sediment melting rather than fluid fluxing. Ba tends to be incompatible regardless of whether the process is sediment melting or sediment dehydration, but Th varies from compatible (immobile) in aqueous fluids to incompatible (mobile) during sediment melting (Johnson and Plank, 1999). Therefore, a high Th/Nb for a given Ba/Nb, as observed for Monte Arcuentu, is consistent with metasomatism of the mantle source via sediment melting.

Nature of the Subducted Sediment

To further constrain the nature of the subducted sediment, we need to place some constraints on the isotopic composition of the mantle source prior to metasomatism. Pb isotope data rule out a mantle source like that giving rise to Etna or the Iblean Plateau. Conversely, while Pb isotope data appear to rule out the depleted mantle (DM) end-member as the source for the Monte Arcuentu rocks, a slightly more radiogenic DM source, like that of some Tyrrhenian Sea basalts, is consistent with the low $^{206}Pb/^{204}Pb$ end of the Monte Arcuentu vertical array (Fig. 7A). We, therefore, model possible mixing scenarios between Tyrrhenian Sea-type mantle and subducted sediment using Sr, Nd, and Hf isotope data (Figs. 11 and 12).

Miocene to Quaternary sediments from the central and eastern Mediterranean (Klaver et al., 2015) have been well characterized in terms of Sr, Nd,

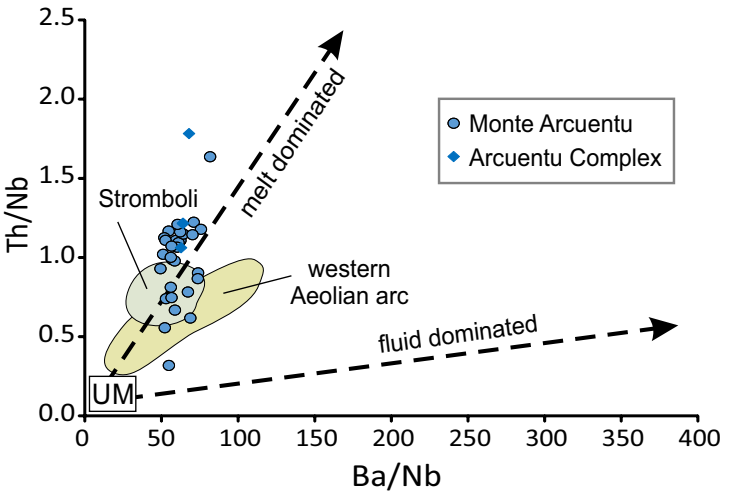

Figure 10. Plot of Th/Nb versus Ba/Nb, modified from Zamboni et al. (2016). UM—upper mantle.

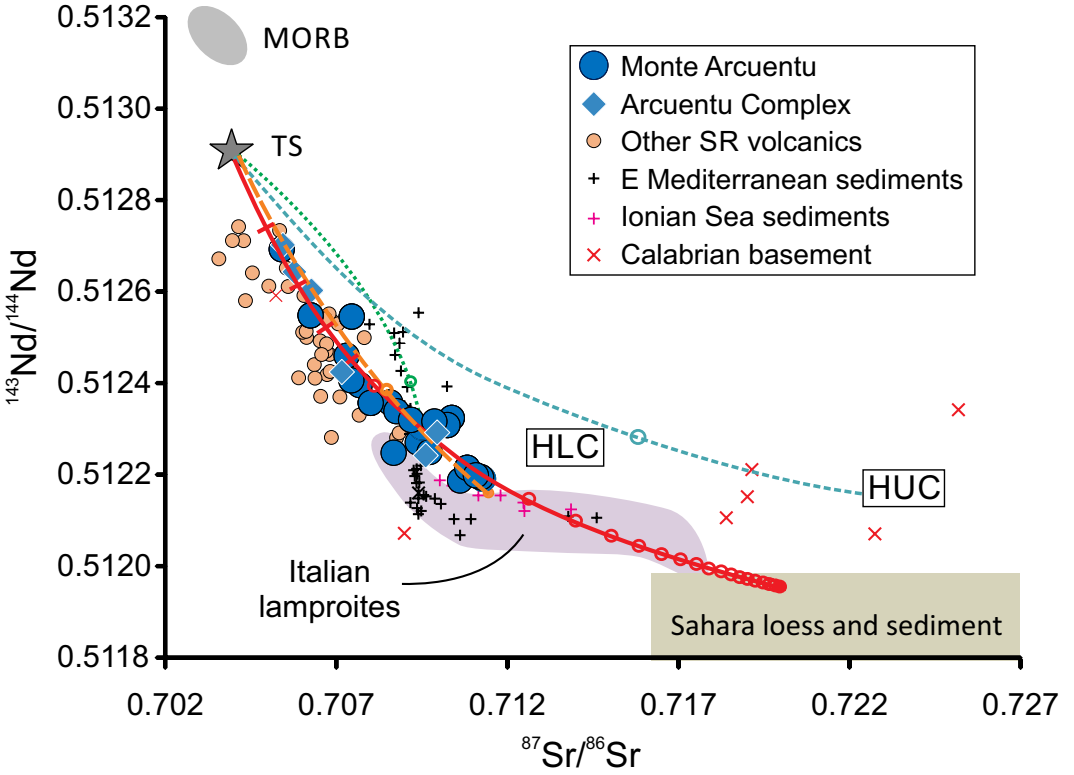

Figure 11. Plot of $^{143}Nd/^{144}Nd$ versus $^{87}Sr/^{86}Sr$ showing results of representative mixing calculations. The solid red curve represents mixing between Tyrrhenian Sea (TS) mantle and Sahara sediment; circles on this curve denote increments of 5% mixing; 1% divisions are shown as tick marks over the first 5% mixing interval. The isotopic composition of TS is inferred from Tyrrhenian Sea basalt data (Beccaluva et al., 1990): $^{87}Sr/^{86}Sr$ = 0.70393, $^{143}Nd/^{144}Nd$ = 0.51291, Sr = 21.1 ppm, Nd = 1.35 ppm. Isotopic values for Sahara sediment are based on the west Sahara potential source area defined by Scheuvens et al. (2013) with elemental concentrations estimated from Grousset et al. (1998): $^{87}Sr/^{86}Sr$ = 0.720, $^{143}Nd/^{144}Nd$ = 0.51195, Sr = 142 ppm, Nd = 30.2 ppm. The dotted green curve represents mixing between average TS mantle and Eastern Mediterranean sediments from Klaver et al. (2015): $^{87}Sr/^{86}Sr$ = 0.70954, $^{143}Nd/^{144}Nd$ = 0.51227, Sr = 834 ppm, Nd = 21.7 ppm. The dashed orange curve represents mixing between average TS mantle and Ionian Sea sediments (Kempton, unpublished data): $^{87}Sr/^{86}Sr$ = 0.71147, $^{143}Nd/^{144}Nd$ = 0.51216, Sr = 282 ppm, Nd = 28 ppm. The dotted blue curve represents mixing between average TS mantle and average Hercynian Upper Crust (HUC) calculated from data in Downes et al. (1997): $^{87}Sr/^{86}Sr$ = 0.72315, $^{143}Nd/^{144}Nd$ = 0.512148, Sr = 138 ppm, Nd = 26 ppm; only the first 10% mixing interval is indicated for the Eastern Mediterranean, Ionian, and Hercynian Upper Crust curves. Shown for reference is the average composition of Hercynian Lower Crust (HLC) calculated from lower crustal xenolith data in Downes et al. (1990, 1991). Other data sources as in Table A1. MORB—mid-oceanic ridge basalt.

Pb, and Hf isotopes; however, Figure 11 shows that, on average, the Sr-Nd isotope compositions of these sediments are too low and too high, respectively, to serve as the contaminant required by the Monte Arcuentu array. This is in part because of their high-biogenic carbonate content (Klaver et al., 2015). Such sediments tend to have $^{87}Sr/^{86}Sr$ values that are limited by the composition of seawater (~0.709 or less), which is considerably lower than the most radiogenic Monte Arcuentu samples (~0.711). Fluvial input from the Nile also tends to have relatively unradiogenic Sr and Pb isotope compositions combined with radiogenic Nd-Hf isotope ratios (Klaver et al., 2015). As a result, contamination of the mantle source by sediments like those in the eastern Mediterranean is unable to explain the full range of Sr-Nd-Pb-Hf isotope compositions at Monte Arcuentu. Sediments from farther west in the Ionian Sea have slightly higher $^{87}Sr/^{86}Sr$ (~0.7115), but their $^{143}Nd/^{144}Nd$ and $^{176}Hf/^{177}Hf$ values overlap the enriched end of the Monte Arcuentu data (Figs. 11 and 12). Thus, the amount of mantle contamination that would be required would be unrealistically large, i.e., >80%, to explain the most enriched samples (Fig. 11). Their $^{207}Pb/^{204}Pb$ values are also too low to explain the compositional range of Monte Arcuentu rocks (Fig. 7B).

An alternative source for the subducted sediment component could be Hercynian-age rocks of Europe. However, mixing curves calculated between Tyrrhenian Sea-type mantle and examples of Hercynian crust (Downes et al., 1997) do not pass through the data (Fig. 11).

Klaver et al. (2015) reported a few Mediterranean sediments with higher $^{87}Sr/^{86}Sr$ values (up to 0.7146), as well as lower $^{143}Nd/^{144}Nd$ (down to 0.51207) and noted that the abundance of this component increases westward. They interpreted this as evidence for an increased contribution from Sahara dust at these sites. If we assume a subducted sediment composition dominated by dust from the western Sahara (Grousset et al., 1998; Scheuvens et al., 2013), the resulting mixing curve reproduces the Monte Arcuentu Sr-Nd isotope array (Fig. 11). Less than 3% sediment addition is required to explain the most primitive (MgO >8.5 wt%) compositions and <12% to encompass the full range of analyses. Given Sardinia's location in the western Mediterranean, it is not unrealistic to assume that sediments of this type dominated the subducted component beneath Sardinia.

Hf isotope data, however, indicate that the subducted sediment component is unlikely to consist of Sahara dust alone, as Sahara-derived aerosols tend

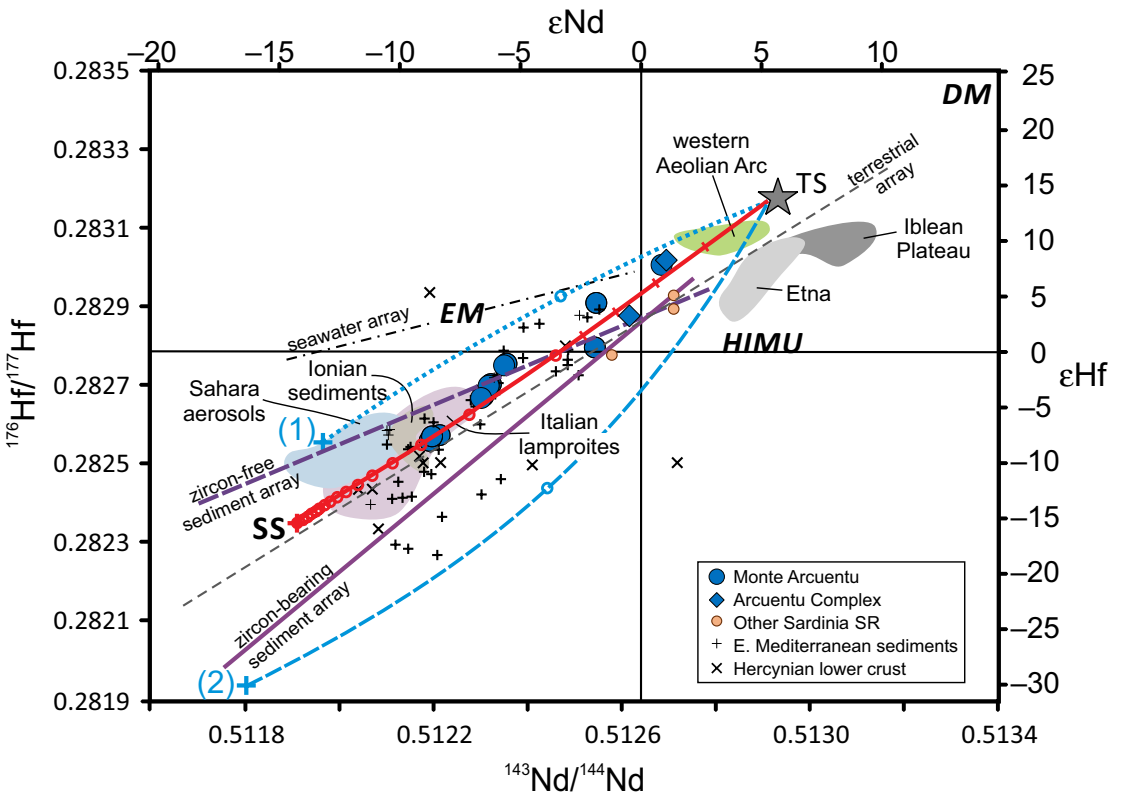

Figure 12. Plot of $^{176}Hf/^{177}Hf$ versus $^{143}Nd/^{144}Nd$ showing results of representative mixing calculations between average Tyrrhenian Sea mantle (TS) and Sahara sediment (SS). Shown for reference are the Terrestrial Array of Vervoort et al. (2011), and the "zircon-free sediment," and "zircon-bearing sediment" arrays from Bayon et al. (2009). The field for Sahara aerosols (Pourmand et al., 2014) overlaps the "zircon-free sediment" array. Results of three mixing calculations are shown: TS-mantle contaminated by (1) zircon-poor sediment or aerosols, i.e., Sahara dust (blue dotted line); (2) zircon-bearing sediment (blue dashed line); and a 2:1 mix of (1) and (2) labeled SS for model Saharan Sediment. Hf isotope composition of TS is inferred from Tyrrhenian Sea basalts (Gasperini et al., 2002): $^{176}Hf/^{177}Hf = 0.28317$, Hf = 0.31 ppm; TS Nd isotope composition as in Figure 11. Zircon-poor sediment composition for western Sahara inferred from Bayon et al. (2009) data for fine-grained sediments from the Congo basin: $^{143}Nd/^{144}Nd = 0.511962$, $^{176}Hf/^{177}Hf = 0.282557$, Nd = 22.44 ppm, Hf = 3.71ppm. Zircon-bearing sediment composition based on coarse-grained shelf sediments from the Congo basin (Bayon et al., 2009): $^{143}Nd/^{144}Nd = 0.511791$, $^{176}Hf/^{177}Hf = 0.281939$, Nd = 18.97 ppm, Hf = 8.30 ppm. Model west Sahara sediment, i.e., 2:1 mix of (1) and (2): $^{143}Nd/^{144}Nd = 0.511906$, $^{176}Hf/^{177}Hf = 0.282353$, Nd = 21.29 ppm, Hf = 5.23 ppm. Other data sources as listed in Table A1. Only the first 5% mixing interval is indicated for the zircon-poor and zircon-bearing sediment mixing curves. Mantle end-members are the same as in Figure 6.

to have radiogenic $^{176}Hf/^{177}Hf$ for a given $^{143}Nd/^{144}Nd$ (Pourmand et al., 2014), and plot significantly above the terrestrial array (Fig. 12). Bayon et al. (2009) found that the Nd and Hf isotope systems are decoupled during continental weathering and sediment transport. Nd isotopes are not significantly fractionated during these processes, but a major fraction of Hf is hosted in zircon, which tends to be sorted into silt and sand fractions during sediment transport (Patchett et al., 1984). As a result, weathering and sediment transport produce two distinct arrays in the εHf versus εNd diagram: a "zircon-bearing sediment array" and a "zircon-free sediment array" (Fig. 12). Mixing calculations involving these two end-members suggest that neither extreme can explain the Monte Arcuentu data array: Contamination by zircon-poor sediment produces a concave downward curve, whereas zircon-bearing sediment produces a concave upward curve (Fig. 12). However, a mixture of fine- and coarse-grained sediment produces a curve that passes through the data, suggesting the sediment contributing to the metasomatism of the Monte Arcuentu mantle was a mixture of both fine-grained, zircon-free sediment, and coarser, zircon-bearing continental shelf-type sediments.

Consistent with the interpretation that the sediment contaminant was terrigenous in origin is the good correlation ($R^2 = 0.8$) exhibited by Monte Arcuentu samples in a plot of $^{176}Lu/^{177}Hf$ versus $^{146}Sm/^{144}Nd$ (Fig. 13), where the data overlap the fields for turbidites and terrestrial clays. By comparison, hydrogenetic and hydrothermal sediments extend to significantly higher $^{176}Lu/^{177}Hf$ values not observed at Monte Arcuentu.

Therefore, Sr-Nd-Hf isotope data are consistent with a model in which the sediments involved in metasomatism of the Monte Arcuentu mantle source were (*i*) predominantly terrigenous in origin, (*ii*) derived from Archean terranes of northern Africa, and (*iii*) contributed to the mantle wedge through melting rather than dehydration.

Pb isotope analyses of Saharan sediments are limited, and aerosols, even from remote areas, are at least partly of anthropogenic origin (Abouchami et al., 2013; Kumar et al., 2014). Nonetheless, available data appear to be inconsistent with the mixing model proposed above based on Sr-Nd-Hf isotopes. Surface sediments from the Bodélé Depression, thought to be one of the largest sources of Saharan dust (Abouchami et al., 2013), have Pb isotope

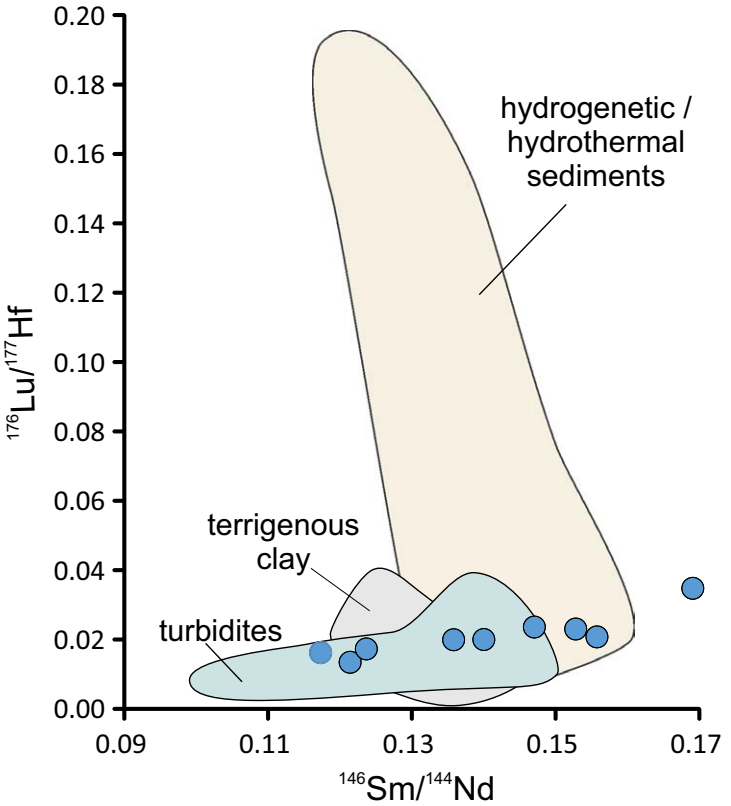

Figure 13. Plot of $^{176}Lu/^{177}Hf$ versus $^{146}Sm/^{144}Nd$ modified from Vervoort et al. (2011).

compositions that are more radiogenic than most sediments from the eastern Mediterranean ($^{206}Pb/^{204}Pb$ >18.9). If representative of the full range of compositions for Sahara aerosols and sediments, they cannot explain the Monte Arcuentu data, particularly the rocks that have high $^{207}Pb/^{204}Pb$ and $^{208}Pb/^{204}Pb$ at low $^{206}Pb/^{204}Pb$ (Figs. 7B and 8B). Thus, the full range of Pb isotope data for Monte Arcuentu cannot be explained by mantle metasomatism alone in response to subduction of any known sediments.

A Case for Both Source Enrichment and Crustal Contamination?

The analysis above suggests that, while source contamination can explain some of the compositional variation in the Monte Arcuentu rocks, neither source metasomatism nor crustal contamination alone can explain the full range of major element, trace element and isotope compositions observed. In order to resolve this conundrum, we revisit the major and trace element characteristics of the Arcuentu rocks. Most of the lavas are too evolved to have equilibrated directly with mantle peridotite. MgO contents are as low as 2.4 wt%, requiring significant amounts of differentiation of primitive magmas to explain these evolved compositions (e.g., Toothill et al., 2007; Melekhova et al., 2015). Yet, we show in Figure 5 that, except for two andesites, most Arcuentu rocks have less than 58 wt% SiO_2, and correlations between SiO_2 and most major and trace elements tend to be weak—variations that differ from many of the orogenic volcanic suites from Sardinia.

In contrast, many of these elements show significant correlations with MgO (Fig. 14)—Al_2O_3, TiO_2, and Sr increase with decreasing MgO, whereas most other Sardinia SR rocks show scattered but broadly positive correlations. Furthermore, Monte Arcuentu rocks that have the lowest MgO contents tend to have the highest $^{87}Sr/^{86}Sr$ and $^{207}Pb/^{204}Pb$, and lowest $^{143}Nd/^{144}Nd$ and $^{176}Hf/^{177}Hf$ values, i.e., isotope variations broadly correlate with indices of magmatic differentiation (Figs. 15A and 15B). Although weak correlations are observed between SiO_2 and most major and trace elements (Fig. 5), SiO_2 correlates positively with $^{207}Pb/^{204}Pb$ and negatively with $^{143}Nd/^{144}Nd$ (and $^{176}Hf/^{177}Hf$) (Figs. 16A and 16B), similar to the correlation observed between SiO_2 and $^{87}Sr/^{86}Sr$ (Figs. 9 and 16C). These trends suggest a role for assimilation-fractional crystallization (AFC) processes, but different from those recorded by most orogenic volcanic rocks (e.g., Figs. 9A and 9B; Fig. S3 [footnote 1]).

The limited range in SiO_2 within the Monte Arcuentu suite indicates that either the magmas underwent limited fractional crystallization or that SiO_2 was buffered during the process. MgO contents as low as 2.8 wt% (for rocks with ~52 wt% SiO_2) confirm that fractional crystallization has occurred. The positive correlation between MgO and Ni (Fig. 14C), and the wide range in Ni contents can be modeled as the result of ~10%–15% olivine fractionation, depending on the D-value assumed; and while the Ni concentrations observed are relatively high for arc rocks, they are lower than in melts in equilibrium with primitive mantle (e.g., ~400–500 ppm). Fractionation of ~30% olivine would be required to account for this compositional range, assuming a parental magma originally in equilibrium with the mantle. Yet, olivine fractionation alone will quickly drive up the SiO_2 concentration of the residual melt due to the low SiO_2 content of olivine, a feature not observed at Monte Arcuentu (Fig. 2).

Therefore, the fractionating assemblage must have been a combination of phases with a bulk solid SiO_2 composition similar to that of the parental melt. The observed increases in TiO_2 and Al_2O_3 (and Sr) with increasing degree of fractionation (Fig. 14) indicate that Fe-Ti oxides and plagioclase were not significant fractionating phases. The absence of plagioclase in the fractionating assemblage suggests that the Monte Arcuentu rocks evolved over a range of near-Moho and lower-crustal depths, i.e., pressures higher than the stability of plagioclase, similar to the Lesser Antilles (Melekhova et al., 2015).

Mafic cumulates consisting of varying proportions of Fe- and Al-rich clinopyroxene and olivine are common in lower crustal xenolith suites (Kempton, 1987; Kempton and Dungan, 1989; Cigolini, 2007; Perinelli et al., 2017). Indeed, Muroi and Arai (2014) report a suite of wehrlites, clinopyroxenites and dunites,

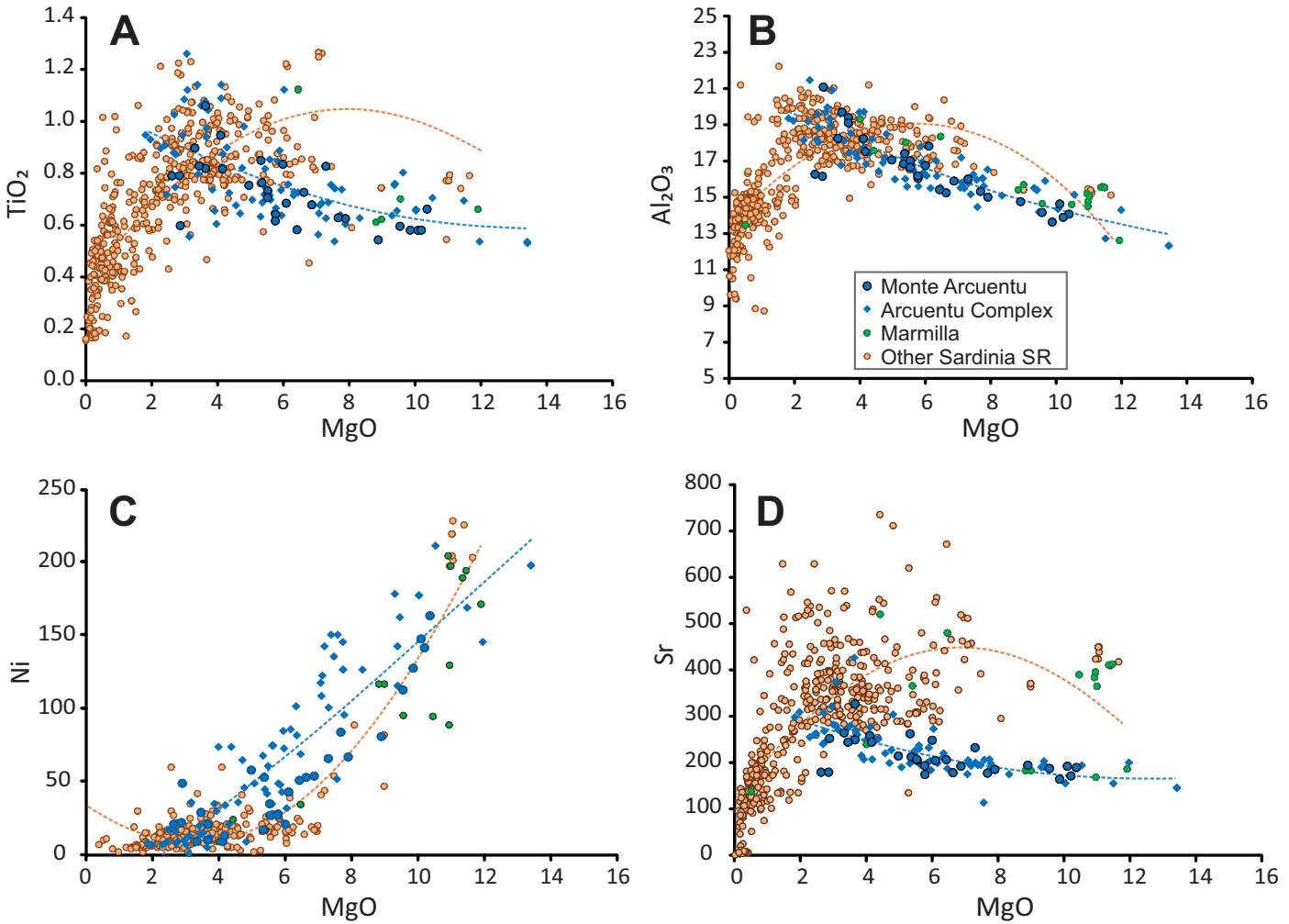

Figure 14. Selected major and trace elements versus MgO for Monte Arcuentu and other SR rocks of Sardinia. In these diagrams, samples from Marmilla are distinguished from other SR rocks (green dots) to note geochemical similarity between this locality and Monte Arcuentu. Curves are best fit second order polynomial to the Monte Arcuentu (blue) and other SR rocks (brown). Data sources as in Figure 2.

which they interpret as cumulates from the sub-arc Moho. The crystallization sequence implied by these xenoliths is distinct from that of olivine-saturated magmas at low pressure and involves a process whereby olivine- and clinopyroxene-oversaturated melts fluctuate around the olivine-clinopyroxene cotectic as the melts evolve, resulting in the crystallization of abundant wehrlites, clinopyroxenites, and dunites in the upper mantle and lower crust.

Depending on the proportion of clinopyroxene to olivine, such fractionating assemblages would not significantly increase the SiO_2 of the residual liquid, but would result in significant magmatic differentiation, driving liquids to low MgO contents, as well as low Ni and Cr. The roughly constant CaO contents of Monte Arcuentu rocks as a function of MgO (Fig. S5A [footnote 1]) suggest that clinopyroxene and olivine fractionated in roughly equal proportions.

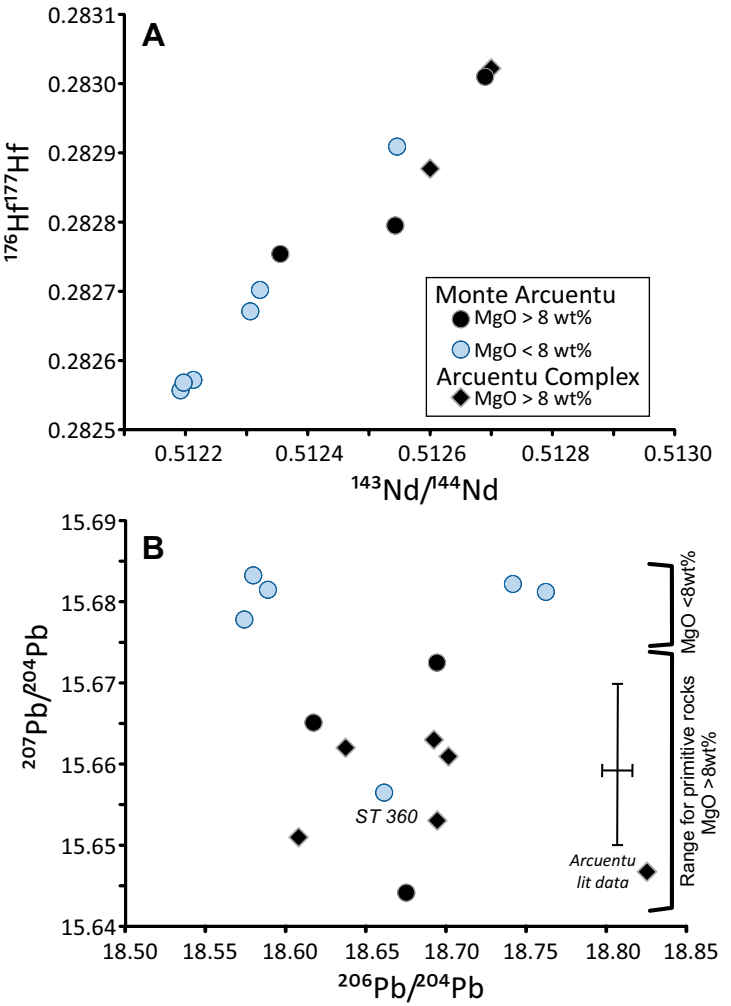

Figure 15. (A) $^{176}Hf/^{177}Hf$ versus $^{143}Nd/^{144}Nd$ for Monte Arcuentu showing the compositional ranges for primitive (MgO >8 wt%) relative to more evolved (MgO <8 wt%) rocks. Lowest isotope ratios are restricted to rocks with less than 6 wt% MgO. (B) $^{207}Pb/^{204}Pb$ versus $^{206}Pb/^{204}Pb$ for Monte Arcuentu, showing the compositional ranges for primitive (MgO >8 wt%) relative to more evolved (MgO <8 wt%) rocks. Note that the older literature data (shown as dark blue diamonds) are all from the more primitive end of the compositional range. Analytical uncertainties were not provided for these older data, but a typical range for analyses by thermal ionization techniques is shown for reference, indicated on the figure as Arcuentu lit data. By comparison, the analytical uncertainties for the new high-precision Pb isotope data reported here are within the size of the symbols. Data for both diagrams from this study and Lustrino et al. (2013). Sample ST360 has a low MgO concentration due to plagioclase accumulation (Downes et al., 2001).

An implication of this scenario is that Monte Arcuentu parental magmas stalled near the Moho, where they potentially interacted with, and became contaminated by, lithospheric mantle and/or mafic lower crust. Assimilation of mafic lower crust has often been discounted on thermodynamic grounds, but thermodynamic modeling studies (Annen and Sparks, 2002; Dufek and Bergantz, 2005; Annen et al., 2006; Solano et al., 2012) have shown that, for high rates of melt accumulation and high melt fractions, repeated overlapping basaltic intrusions into a deep "hot zone" at the base of the crust allows melt to remain compositionally stable for long periods. Each increment of basalt intrusion into the deep "hot zone" can generate partial melting of surrounding rocks due to heat transfer, with the nature of the resulting hybrid melt depending on the spectrum of lithologies available in the portion of lithosphere (crust or mantle) intruded (e.g., Gao et al., 2016) and the details of the AFC process.

Isotope and trace element variations in the Monte Arcuentu suite provide us with geochemical evidence for the nature of these deep crust/upper mantle interactions without the geochemical overprinting of mid- to upper crustal AFC processes seen in most other orogenic suites. The variations in Nd, Sr, and Hf isotopes are somewhat less sensitive in this context, because lithospheric mantle and lower crust tend to plot in similar parts of the isotope diagrams (Figs. 6, 11, and 12), but Pb isotope variations and some key trace element ratios are more illuminating.

Assuming that the most primitive basalt compositions have undergone limited fractional crystallization and crustal contamination, we can infer that their isotopic variability reflects the compositional heterogeneity of the enriched mantle source, i.e., metasomatized by melts derived from recycling of sediments dominated by Sahara sediment. The most primitive rocks at Monte Arcuentu (MgO >8.5 wt %) have a range for $^{87}Sr/^{86}Sr$ up to 0.709, with $^{143}Nd/^{144}Nd$ and $^{176}Hf/^{177}Hf$ values down to 0.5123 and 0.2828, respectively, and $^{207}Pb/^{204}Pb$ values up to 15.673 (Fig. 16). Therefore, isotope compositions outside this range must be the product of interactions with the crust and/or lithospheric mantle.

Figures 7B and 15B suggest that interaction with lower crust similar to the Hercynian basement rocks of Calabria is responsible for the evolved Monte Arcuentu rocks with high $^{207}Pb/^{204}Pb$ and low $^{206}Pb/^{204}Pb$. This is not unreasonable, since Calabria was in crustal continuity with Sardinia–Corsica prior to the opening of the Tyrrhenian Sea (Fig. 1B) (Carminati et al., 2010, 2012). The contaminant for the evolved Monte Arcuentu rocks with high $^{207}Pb/^{204}Pb$–high $^{206}Pb/^{204}Pb$ is less clear, but the overlap with compositions of Italian lamproites and other potassic volcanic rocks of central Italy suggest that their parental magmas may have interacted with lithospheric mantle.

This interpretation is supported by variations in key trace element ratios, such as Rb/Ba, which in the Monte Arcuentu rocks correlate with Pb isotope ratios, i.e., rocks with high $^{206}Pb/^{204}Pb$ have high Rb/Ba, whereas those with lower $^{206}Pb/^{204}Pb$ have lower Rb/Ba (Fig. 17A). This is significant because lower crust typically has a low Rb/Ba ratio, as shown by Hercynian lower crustal

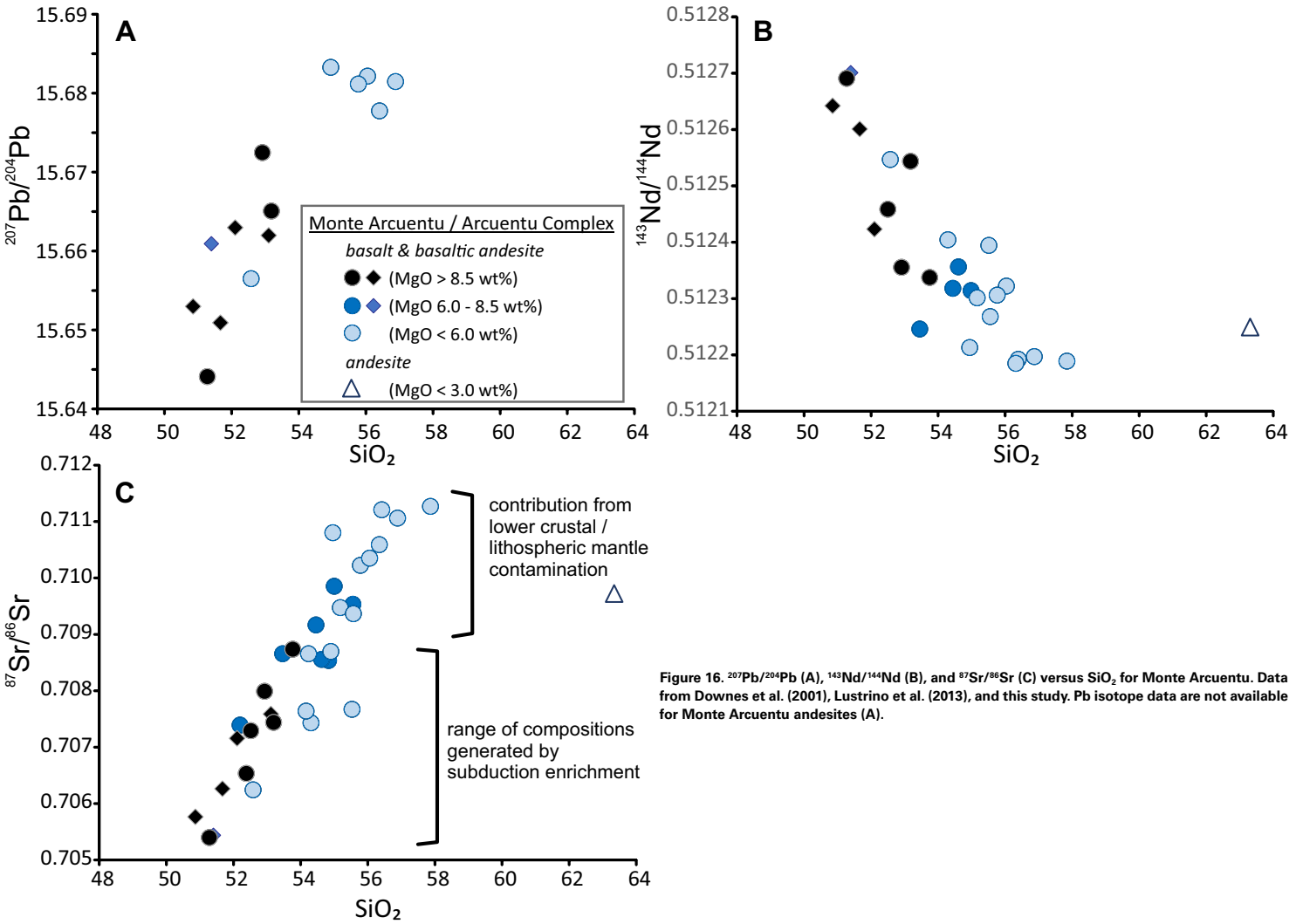

Figure 16. $^{207}Pb/^{204}Pb$ (A), $^{143}Nd/^{144}Nd$ (B), and $^{87}Sr/^{86}Sr$ (C) versus SiO_2 for Monte Arcuentu. Data from Downes et al. (2001), Lustrino et al. (2013), and this study. Pb isotope data are not available for Monte Arcuentu andesites (A).

xenoliths of Europe (Downes et al., 1991) and Calabrian basement (Caggianelli et al., 1991). Upper crust is distinguished by having much higher Rb/Ba, e.g., most Hercynian granitoids (Downes et al., 1997) have Rb/Ba ratios >0.2. The lithospheric mantle is likely to be heterogeneous, depending on age and geologic history, but we can infer that in the Mediterranean region its Rb/Ba ratio is likely to be high. Italian lamproites, for example, have Rb/Ba ratios up to 0.65 (Fig. 17A; Prelević et al., 2010). The lamproite from Sisco, Corsica, France—the nearest lamproite locality to Monte Arcuentu in time and space—has both high Rb/Ba (0.34) and high Pb isotope ratios ($^{206}Pb/^{204}Pb$ = 18.85, $^{207}Pb/^{204}Pb$ = 15.7).

Further support for this interpretation is provided by the variation in $^{143}Nd/^{144}Nd$ versus Rb/Ba (Fig. 17B). High MgO rocks from Monte Arcuentu have a limited range of Rb/Ba ratios with $^{143}Nd/^{144}Nd$ values of 0.5123–0.5127. More evolved rocks separate into two groups, the low Rb/Ba–low $^{143}Nd/^{144}Nd$ (and low $^{206}Pb/^{204}Pb$) group trend toward the compositions of lower crust,

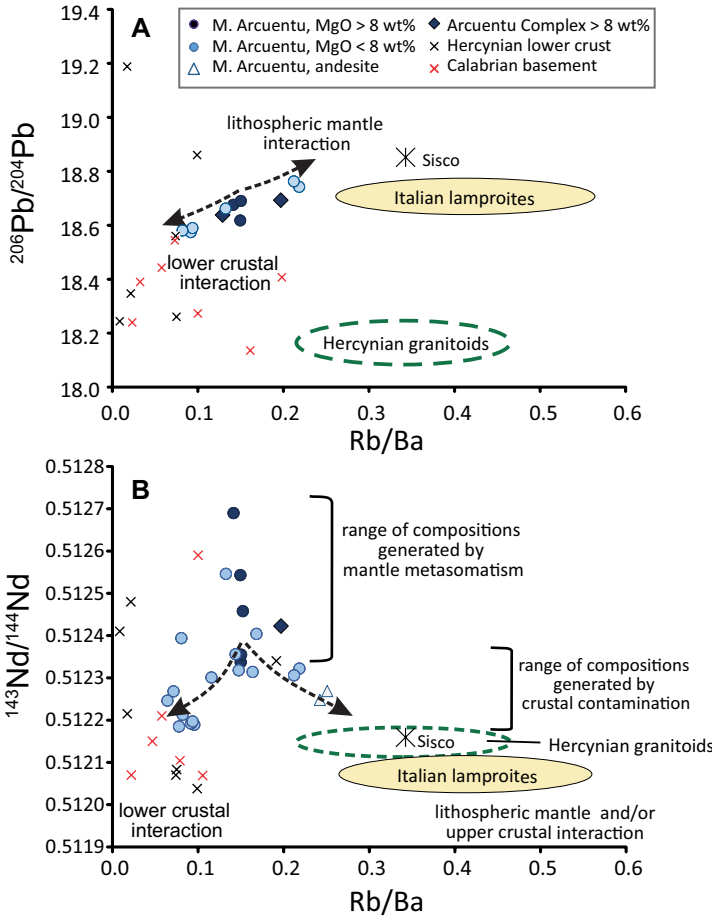

Figure 17. Plot of Rb/Ba vs (A) $^{206}Pb/^{204}Pb$ and (B) $^{143}Nd/^{144}Nd$ for Monte Arcuentu, showing compositional ranges for primitive (MgO >8.5 wt%) relative to more evolved rocks (MgO <8.5 wt%). Ellipses for Italian lamproites and Hercynian granitoids represent one standard deviation from the mean composition. Data sources as listed in Table A1.

supporting the interpretation that their parental magmas interacted with lower crustal lithologies. The high Rb/Ba group trends toward the fields for Hercynian granitoids (upper crust) and lithospheric mantle. Because upper crust and lithospheric mantle plot in roughly the same part of the diagram, we cannot distinguish them based on Figure 17B. However, the variations in $^{206}Pb/^{204}Pb$ versus Rb/Ba (Fig. 17A) clearly show that upper crustal contamination is unlikely, because of its much lower $^{206}Pb/^{204}Pb$ (and $^{207}Pb/^{204}Pb$; Downes et al., 1997).

Proposed Model for the Origin of Monte Arcuentu Magmas

Figure 18 summarizes the proposed model for the origin of Monte Arcuentu rocks, which are unique among Sardinia SR rocks. Lower Al_2O_3, TiO_2, P_2O_5, and higher Ni and Cr for a given SiO_2 or MgO, suggest that the Monte Arcuentu mantle source was more depleted than that giving rise to other Sardinian SR rocks (Figs. 5, 14, S2 [footnote 1], and S4). Sr, Nd, Pb, and Hf isotopes, however, provide evidence for time-integrated enrichment relative to DM, suggesting a source that was more akin to that of Tyrrhenian Sea tholeiites (Fig. 7).

The mantle source was metasomatized by partial melts derived from subducted sediments that were predominantly terrigenous and derived from Archean terranes of northern Africa. This metasomatized mantle source can explain the range of isotope signatures observed in high-MgO basaltic rocks but not the full range of isotopic compositions (Figs. 6, 7, and 8). Mixing calculations suggest that less than 3% source contamination is needed to account for the Sr, Nd, and Hf compositions of the most primitive rocks (Figs. 11 and 12).

In contrast to most other orogenic settings, most of the Monte Arcuentu parental magmas stalled at the base of the crust or at the top of the lithospheric mantle on their way to the surface and underwent MASH-type processes (Hildreth and Moorbath, 1988). As a result, we envisage four possible scenarios to explain the geochemical evolution of the Monte Arcuentu magmas.

(1) Melts escaped to the surface with minimal interaction with crust or lithospheric mantle, preserving the isotopic signature of the metasomatized mantle source. Some of the most primitive rocks may fall into this category. They exhibit a range of $^{87}Sr/^{86}Sr$ values up to 0.709, $^{143}Nd/^{144}Nd$ and $^{176}Hf/^{177}Hf$ values down to 0.5123 and 0.2828, respectively, and $^{207}Pb/^{204}Pb$ values up to 15.673.

(2) Melts ponded at the Moho and interacted with enriched lithospheric mantle. They evolved to low MgO, low Ni and Cr contents as a result of olivine and clinopyroxene fractionation and underwent limited enrichment in SiO_2. These melts erupted with higher $^{207}Pb/^{204}Pb$, $^{87}Sr/^{86}Sr$, and Rb/Ba, and lower $^{143}Nd/^{144}Nd$ and $^{176}Hf/^{177}Hf$ than the primitive lavas of (1). Italian lamproites provide an indication of the composition of the lithospheric mantle in this scenario.

(3) Melts ponded within the lower crust and interacted with lithologies similar to Calabrian basement or Hercynian lower crust. These melts are compositionally similar to (2) but are distinguished by their lower $^{206}Pb/^{204}Pb$ and Rb/Ba, inherited from interaction with these older rocks (Fig. 17B).

(4) Melts ponded within and interacted with mid- to upper crust, evolving to higher SiO_2 and Rb/Ba; $^{87}Sr/^{86}Sr$ and $^{143}Nd/^{144}Nd$ compositions overlap the range of evolved Monte Arcuentu lavas. We have no Pb or Hf analyses of the two Monte Arcuentu andesites, so we do not know precisely how mid- to upper crustal AFC processes affected these isotope

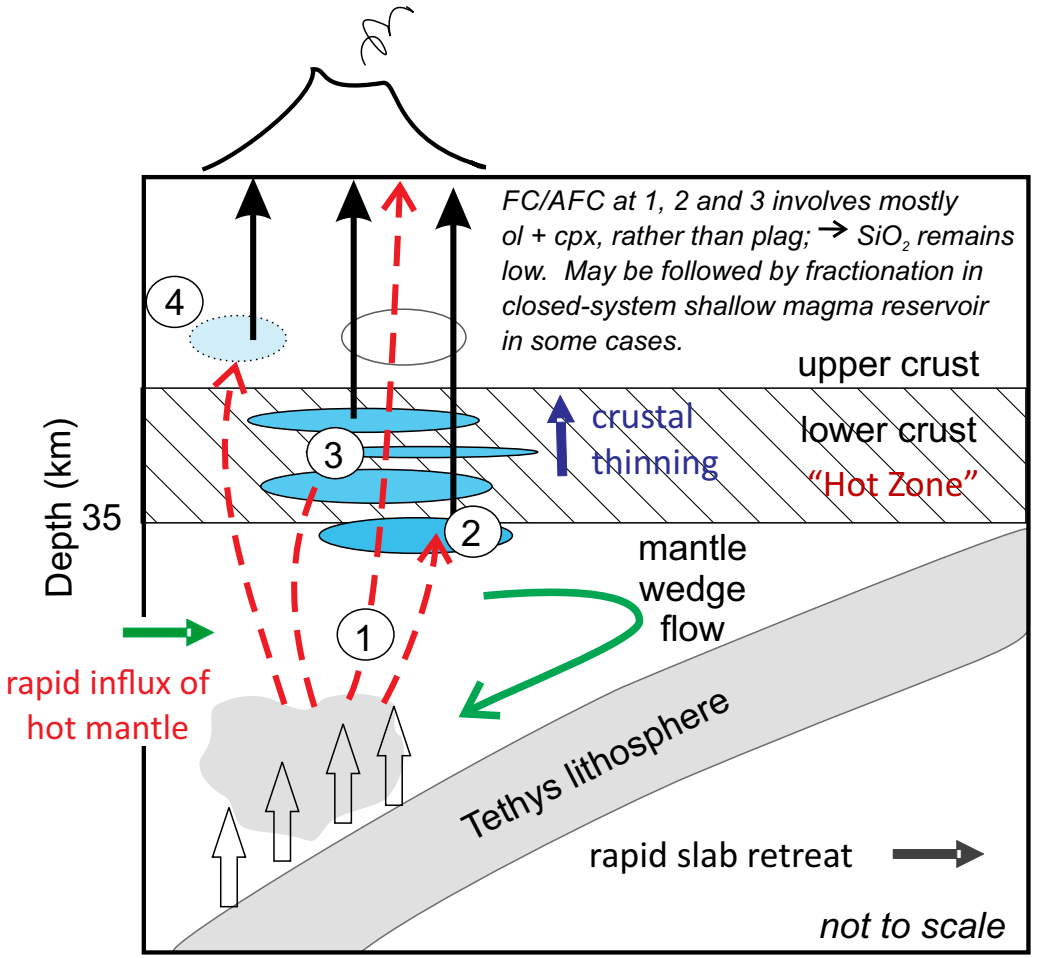

Figure 18. Proposed model for the origin and evolution of Monte Arcuentu orogenic magmatism. Numbers correspond to the four scenarios discussed in the text. FC—fractional crystallization; AFC—assimilation–fractional crystallization; ol + cpx—olivine + clinopyroxene; plag—plagioclase.

ratios. However, based on data for other Sardinia SR rocks, $^{207}Pb/^{204}Pb$ is likely to be lower than in the melts contaminated by both lithospheric mantle and lower crust.

Aside from scenario 4, we have so far ignored the effects of shallow level magma chamber processes. However, rocks from Arcuentu are commonly porphyritic, including the presence of plagioclase phenocrysts (Brotzu et al., 1997). Presence of this relatively low-pressure phase is seemingly at odds with most of the scenarios above. However, Brotzu et al. (1997) used major and trace element modeling to show that shallow-level magma chamber processes affecting the Arcuentu Complex rocks involved fractional crystallization but negligible crustal contamination. Instead, these authors proposed that Arcuentu Complex magmas underwent polybaric fractionation at elevated to moderate pressures, and that the shallow-crustal magma chamber was filled by melts that were already moderately evolved. Therefore, while Arcuentu Complex magmas may have undergone late stage crystallization of plagioclase phenocrysts to varying degrees in shallow crustal magma chambers, this process operated as a closed system and did not obscure key geochemical characteristics inherited from melt interactions that occurred in the lower crust and lithospheric mantle.

The model proposed here for the origin of Monte Arcuentu magmas requires high rates of melt accumulation and high melt fractions in order to

partially melt the lithospheric mantle and lower crust, given the typically refractory nature of these lithologies, but such a scenario is consistent with the rapid rotation and extension that was occurring in southern Sardinia at the time (Montigny et al., 1981; Morra et al., 1997; Mattioli et al., 2000; Gattacceca et al., 2007; Carminati et al., 2012). The Sardinia–Corsica complex is also one of the few places in the western Mediterranean where geophysical data confirm the existence of mechanically non-competent crustal layers (Splendore and Marotta, 2013). These authors estimate that up to 50% of the upper crust and up to 100% of the lower crust are non-competent. There is also a rapid decrease in strength, up to two or three orders of magnitude, below the Sardinia–Corsica complex (Splendore and Marotta, 2013).

The fact that Monte Arcuentu may represent some of the latest stages of orogenic magmatism on Sardinia may have contributed to the predominance of lower crustal/upper mantle interactions. Earlier phases of orogenic magmatism would have provided the heat needed to "soften" the lower crust, making it possible for assimilation of these otherwise refractory lithologies over time. Furthermore, the tectonic conditions following rotation of Sardinia at 18 Ma, i.e., high rates of extension, may have facilitated more rapid ascent of magmas with minimal interaction with mid- to upper crust (Morra et al., 1997; Mattioli et al., 2000). This clearly contrasts with the petrogenesis of most other Sardinia SR rocks, which appear to have differentiated and assimilated larger proportions of middle to upper crust (Guarino et al., 2011; Lustrino et al., 2013).

Whether the mantle-derived melts interact with pre-existing (old) crust or basalts/gabbros from earlier melt injection events may relate to crustal structure and/or length of time over which magmatism has occurred. Geophysical data suggest that the overall crustal thickness of Sardinia is similar north to south, with the north slightly thicker (Splendore and Marotta, 2013). However, the upper crust is believed to be thicker than the lower crust in the north, whereas the reverse is true for the south where the lower crust is thicker. It is intriguing to speculate whether this thicker lower crust in southern Sardinia is the cause or the outcome of the petrogenetic model proposed here, i.e., Monte Arcuentu lavas predominantly ponding and crystallizing in the lower crust, thickening it, or whether a thicker lower crust presented a greater barrier to ascent, forcing more magmas to stall here in their ascent to the surface. More detailed petrologic study of individual volcanic centers across Sardinia may help to resolve this question.

CONCLUSIONS

- Miocene subduction-related volcanic rocks from Monte Arcuentu, southern Sardinia, are compositionally unique compared with most orogenic magmas. They exhibit a wide range in Sr, Nd, Pb, and Hf isotopic compositions and MgO for a very limited range in SiO_2. These compositional variations reflect AFC processes that occurred mainly in the lower crust and upper mantle where clinopyroxene and olivine were the predominant fractionating phases rather than plagioclase.
- The parental magmas were derived from a mantle source that had been metasomatized by partial melts derived from subducted sediment. Trace element and isotopic ratios for the most primitive rocks (MgO >8 wt%) suggest a high proportion of terrigenous or detrital material within the subducted sediment, most likely derived from the Archean terranes of northern Africa, and contamination of a mantle source similar to that giving rise to Tyrrhenian Sea basalts.
- Because mantle enrichment processes were dominated by sediment melting rather than sediment dehydration, Hf behaved as a mobile, non-conservative element.
- Trace element and isotopic ratios for the more evolved rocks in the suite provide evidence for assimilation of lower crust and/or lithospheric mantle.
- Partial melting of these normally refractory lithologies was facilitated by the rapid phase of extension and rotation of Sardinia during the mid-Miocene.
- The Monte Arcuentu rocks provide insights into assimilation processes in the lower crust and lithospheric mantle that may be obscured by upper crustal AFC processes in other orogenic suites.

ACKNOWLEDGMENTS

PDK and HD acknowledge support from the National Environment Research Council (NERC) Isotope Geosciences Laboratory for the new Pb and Hf isotope data; Ian Millar is thanked for completing the Pb isotope mass spectrometry and Tiffany Barry for completing the Hf isotope mass spectrometry. Angelo Peccerillo and Gianfilippo De Astis are gratefully acknowledged for providing the Ionian Sea sediment samples. Sue Trayhorn and Bob Thompson are recognized for initiating the project and collecting the original samples. ML acknowledges Sapienza Università di Roma (Progetti Ricerca Ateneo 2016 and 2017) financial support. The manuscript benefited from the thoughtful reviews of Nick Rogers and Bob Stern. Thanks to Shan de Silva for his editorial handling.

APPENDIX. ANALYTICAL METHODS

Samples for Pb and Hf isotope analysis were prepared at the NERC Isotope Geosciences Laboratory (NIGL) following procedures outlines in Kempton (1995) and Kempton et al. (2000) for Pb and Hf, respectively. All samples were dissolved from hand-picked chips that were leached in cold, dilute HCL for ~30 min to remove the effects of low temperature alteration, although the low loss on ignition (LOI) for the dike and lava samples (<1.1 wt%; Downes et al., 2001) indicates the rocks are relatively fresh. The LOI for breccia sample ST84 is slightly higher at 1.88 wt%. Pb isotopes were analyzed on a Neptune MC-ICP-MS at Thermo Scientific, Bremen, Germany, using the Tl-doping method to correct for mass fractionation during the run. All Pb isotope ratios have been corrected relative to the NIST NBS 981 composition of Todt et al. (1996). Based on repeated runs of NBS 981, the reproducibility of whole rock Pb isotope measurements is better than ± 0.01% (2σ). Hf isotopes were analyzed on a Neptune MC-ICP-MS at Goethe Universität Frankfurt, Germany. Within-run standard error for Hf isotope measurements is normally less than 22 ppm (2σ). Minimum uncertainties are derived from external precision of standard measurements, which average 43 ppm (2σ). Replicate analysis of internal rock standard, pk-G-D12, over the course of analysis yields 0.283048 ± 12 (2σ, n = 27), which is indistinguishable from previously reported value determined by MC-ICP-MS (Kempton et al., 2000). The data are corrected for mass fractionation during the run by normalization to $^{179}Hf/^{177}Hf$ of 0.7325 and are reported relative to an accepted value of the Hf isotope standard JMC 475 of 0.282160.

TABLE A1. SOURCES OF ISOTOPE DATA USED IN THE CONSTRUCTION OF DIAGRAMS

Isotope ratios	Sr	Nd	Pb	Hf
Sardinia, including Monte Arcuentu				
this study			X	X
Downes et al. (2001)	X	X		
Lustrino et al. (2013) and references therein	X	X	X	X
Etna				
Armienti et al. (1989)	X	X		
Gasperini et al. (2002)			X	X
Spence (2012)	X	X	X	X
Tonarini et al. (1995)	X	X		
Viccaro and Cristofolini (2008)	X	X	X	
Viccaro et al. (2011)				X
Iblean Plateau				
Gasperini et al. (2002)			X	X
Kempton (unpublished data)		X		X
Tonarini et al. (1996)	X	X		
Trua et al. (1998)	X	X	X	
Tyrrhenian Sea				
Beccaluva et al. (1990)	X	X		
Gasperini et al. (2002)			X	X
Trua et al. (2003)	X	X		
Western Aeolian Arc (Alicudi and Filicudi)				
Francalanci et al. (1993)	X	X	X	
Gasperini et al. (2002)				X
Kempton (unpublished data)				X
Peccerillo et al. (1993)	X	X	X	
Peccerillo et al. (2004)	X	X	X	
Santo et al. (2004)	X	X	X	
Vulcano				
De Astis et al. (2000)	X	X	X	
Del Moro et al. (1998)	X	X	X	
Gasperini et al. (2002)				X
Gioncada et al. (2003)	X	X	X	
Stromboli				
Francalanci et al. (1993)	X	X		
Kempton (unpublished data)			X	X
Landi et al. (2009)	X	X		
Campanian Province				
Ayuso et al. (1998)	X	X	X	
Belkin and De Vivo (1993)	X	X	X	
D'Antonio and Di Girolamo (1994)	X	X	X	
D'Antonio et al. (1999)	X	X	X	
De Astis et al. (2006)	X	X	X	
Di Renzo et al. (2007)	X	X	X	
Gasperini et al. (2002)				X
Hawkesworth and Vollmer (1979)	X	X		
Kempton (unpublished data)		X		X
Orsi et al. (1995)	X	X	X	
Pappalardo et al. (2002)	X	X	X	
Ernici & Roccamonfina				
Civetta et al. (1981)	X	X	X	
Conticelli et al. (2009)	X	X	X	
Gasperini et al. (2002)	X	X	X	X
Roman Province				
Conticelli et al. (1997)	X	X		
Fornaseri et al. (1963)	X	X		
Gasperini et al. (2002)	X	X	X	X
Perini et al. (2004)	X	X	X	
Rogers et al. (1985)	X	X		
Italian lamproites				
Conticelli et al. (2013)	X	X	X	
Kempton (unpublished data)	X	X	X	X
Prelević et al. (2010)	X	X	X	X
Eastern Mediterranean Sea sediments				
Klaver et al. (2015)	X	X	X	X
Ionian Sea sediments				
Kempton (unpublished data)	X	X	X	X
Hercynian crust				
Downes et al. (1990, 1991, 1997)	X	X	X	
Vervoort et al. (2000)				X
Calabrian basement				
Caggianelli et al. (1991)	X	X	X	

REFERENCES CITED

Abouchami, W., Nätheb, K., Kumar, A., Galert, S.J.G., Jochum, K.P., Williams, E., Horbe, A.M.C., Rosa, J.W.C., Balsam, W., Adams, D., Mezger, K., and Adreae, M.A., 2013, Geochemical and isotopic characterization of the Bodélé Depression dust source and implications for transatlantic dust transport to the Amazon Basin: Earth and Planetary Science Letters, v. 380, p. 112–123, https://doi.org/10.1016/j.epsl.2013.08.028.

Advokaat, E.L., van Hinsbergen, D.J.J., Maffione, M., Langereis, C.G., Vissers, R.L.M., Cherchi, A., Schroeder, R., Madani, H., and Columbu, S., 2014, Eocene rotation of Sardinia, and the paleogeography of the western Mediterranean region: Earth and Planetary Science Letters, v. 401, p. 183–195, https://doi.org/10.1016/j.epsl.2014.06.012.

Albarède, F., Simonetti, A., Vervoort, J.D., Blichert-Toft, J., and Abouchami, W.A., 1998, A Hf–Nd isotopic correlation in ferromanganese nodules: Geophysical Research Letters, v. 25, p. 3895–3898, https://doi.org/10.1029/1998GL900008.

Annen, C., and Sparks, R.S.J., 2002, Effects of repetitive emplacement of basaltic intrusions on thermal evolution and melt generation in the crust: Earth and Planetary Science Letters, v. 203, p. 937–955, https://doi.org/10.1016/S0012-821X(02)00929-9.

Annen, C., Blundy, J.D., and Sparks, R.S.J., 2006, The genesis of intermediate and silicic magmas in deep crustal hot zones: Journal of Petrology, v. 47, p. 505–539, https://doi.org/10.1093/petrology/egi084.

Armienti, P., Innocenti, F., Petrini, R., Pompilio, M., and Villari, L., 1989, Petrology and Sr-Nd isotope geochemistry of recent lavas from Mt. Etna: Bearing on the volcano feeding system: Journal of Volcanology and Geothermal Research, v. 39, p. 315–327, https://doi.org/10.1016/0377-0273(89)90095-4.

Assorgia, A., Balogh, K., Lecca, L., Ibba, A., Procu, A., Secchi, F., and Tilocca, G., 1995, Volcanological characters and structural context of Oligo-Miocene volcanic successions from Central Sardinia (Italy): Rapporti Alpi Appennino: Accademia Nazionale delle Scienze, v. 14, p. 397–424.

Avanzinelli, R., Lustrino, M., Mattei, M., Melluso, L., and Conticelli, S., 2009, Potassic and ultrapotassic magmatism in the circum-Tyrrhenian region: Significance of carbonated pelitic vs. pelitic sediment recycling at destructive plate margins: Lithos, v. 113, p. 213–227, https://doi.org/10.1016/j.lithos.2009.03.029.

Ayuso, R.A., De Vivo, B., Rolandi, G., Seal, R.R., II, and Paone, A., 1998, Geochemical and isotopic (Nd-Pb-Sr-O) variations bearing on the genesis of volcanic rocks from Vesuvius, Italy: Journal of Volcanology and Geothermal Research, v. 82, p. 53–78, https://doi.org/10.1016/S0377-0273(97)00057-7.

Barry, T.L., Pearce, J.A., Leat, P.T., Millar, I.L., and le Roex, A.P., 2006, Hf isotope evidence for selective mobility of high-field-strength elements in a subduction setting: South Sandwich Islands: Earth and Planetary Science Letters, v. 252, p. 223–244, https://doi.org/10.1016/j.epsl.2006.09.034.

Bayon, G., Burton, K.W., Soulet, G., Vigier, N., Dennielou, B., Etoubleau, J., Ponzevera, E., German, C.R., and Nesbitt, R.W., 2009, Hf and Nd isotopes in marine sediments: Constraints on global silicate weathering: Earth and Planetary Science Letters, v. 277, p. 318–326, https://doi.org/10.1016/j.epsl.2008.10.028.

Beccaluva, L., Civetta, L., Macciotta, G., and Ricci, C.A., 1985, Geochronology in Sardinia: Results and problems: Rendiconti della Società Italiana di Mineralogia e Petrologia, v. 40, p. 57–72.

Beccaluva, L., Bonatti, E., Dupuy, C., Ferrara, G., Innocenti, F., Lucchini, F., Macera, P., Petrini, R., Rossi, P.L., Serri, G., Seyler, M., and Siena, F., 1990, Geochemistry and mineralogy of volcanic rocks from ODP sites 650, 651, 655 and 654 in the Tyrrhenian Sea, *in* Stewart, N.J., ed., Proceedings of the Ocean Drilling Program, Scientific Results: Washington, D.C., U.S. Govt. Print. Office, p. 49–73.

Belkin, H.E., and De Vivo, B., 1993, Fluid inclusion studies of ejected nodules from Plinian eruptions of Mt. Somma–Vesuvius: Journal of Volcanology and Geothermal Research, v. 58, p. 89–100, https://doi.org/10.1016/0377-0273(93)90103-X.

Brotzu, P., Lonis, R., Melluso, L., Morbidelli, L., Traversa, G., and Franciosi, L., 1997, Petrology and evolution of calcalkaline magmas from the Arcuentu volcanic complex (SW Sardinia, Italy): Periodico di Mineralogia, v. 66, p. 151–184.

Caggianelli, A., Del Moro, A., Paglionico, A., Piccarreta, G., Pinarelli, L., and Rottura, A., 1991, Lower crustal granite genesis connected with chemical fractionation in the continental crust of Calabria (Southern Italy): European Journal of Mineralogy, v. 3, p. 159–180, https://doi.org/10.1127/ejm/3/1/0159.

Carminati, E., Lustrino, M., Cuffaro, M., and Doglioni, C., 2010, Tectonics, magmatism and geodynamics of Italy: What we know and what we imagine: Journal of the Virtual Explorer, v. 36, paper 9, https://doi.org/10.3809/jvirtex.2010.00226.

Carminati, E., Lustrino, M., and Doglioni, C., 2012, Geodynamic evolution of the central and western Mediterranean: Tectonics vs. igneous petrology constraints: Tectonophysics, v. 579, p. 173–192, https://doi.org/10.1016/j.tecto.2012.01.026.

Casini, L., Cuccuru, S., Puccini, A., Oggiano, G., and Rossi, Ph., 2015, Evolution of the Corsica–Sardinia Batholith and late-orogenic shearing of the Variscides: Tectonophysics, v. 646, p. 65–78, https://doi.org/10.1016/j.tecto.2015.01.017.

Cigolini, C., 2007, Petrography and thermobarometry of high-pressure ultramafic ejecta from Mount Vesuvius, Italy: Inferences on the deep feeding system: Periodico di Mineralogia, v. 76, p. 5–24.

Civetta, L., Innocenti, F., Manetti, P., Peccerillo, A., and Poli, G., 1981, Geochemical characteristics of potassic volcanics from Mt. Ernici (Southern Latium, Italy): Contributions to Mineralogy and Petrology, v. 78, p. 37–47, https://doi.org/10.1007/BF00371142.

Conte, A.M., Palladino, D.M., Perinelli, C., and Argenti, E., 2010, Petrogenesis of the high-alumina basalt-andesite suite from Sant'Antioco Island, SW Sardinia, Italy: Periodico di Mineralogia, v. 79, p. 27–55.

Conticelli, S., Francalanci, L., Manetti, P., Cioni, R., and Sbrana, A., 1997, Petrology and geochemistry of the ultrapotassic rocks from the Sabatini Volcanic District, central Italy: The role of evolutionary processes in the genesis of variably enriched alkaline magmas: Journal of Volcanology and Geothermal Research, v. 75, p. 107–136, https://doi.org/10.1016/S0377-0273(96)00062-5.

Conticelli, S., Marchionni, S., Rosa, D., Giordano, G., Boari, E., and Avanzinelli, R., 2009, Shoshonite and sub-alkaline magmas from an ultrapotassic volcano: Sr-Nd-Pb isotope data on the Roccamonfina volcanic rocks, Roman Magmatic Province, Southern Italy: Contributions to Mineralogy and Petrology, v. 157, p. 41–63, https://doi.org/10.1007/s00410-008-0319-8.

Conticelli, S., Avanzinelli, R., Poli, G., Braschi, E., and Giordano, G., 2013, Shift from lamproite-like to leucititic rocks: Sr–Nd–Pb isotope data from the Monte Cimino volcanic complex vs. the Vico stratovolcano, Central Italy: Chemical Geology, v. 353, p. 246–266, https://doi.org/10.1016/j.chemgeo.2012.10.018.

D'Antonio, M., and Di Girolamo, P., 1994, Petrological and geochemical study of mafic shoshonitic volcanics from Procida-Vivara and Ventotene islands (Campanian Region, South Italy): Acta Vulcanologica, v. 5, p. 69–80.

D'Antonio, M., Civetta, L., and Di Girolamo, P., 1999, Mantle source heterogeneity in the Campanian Region (South Italy) as inferred from geochemical and isotopic features of mafic volcanic rocks with shoshonitic affinity: Mineralogy and Petrology, v. 67, p. 163–192, https://doi.org/10.1007/BF01161520.

Davidson, J.P., McMillan, N.J., Moorbath, S., Worner, G., Harmon, R.S., and Lopez-Escobar, L., 1990, The Nevados de Payachata volcanic region (18°S/69°W, N. Chile) II. Evidence for widespread crustal involvement in Andean magmatism: Contributions to Mineralogy and Petrology, v. 105, p. 412–432, https://doi.org/10.1007/BF00286829.

De Astis, G., Peccerillo, A., Kempton, P.D., La Volpe, L., and Wu, C., 2000, Transition from calc-alkaline to potassium-rich magmatism in subduction environments: Geochemical and Sr, Nd, Pb isotopic constraints from the Island of Vulcano (Aeolian arc): Contributions to Mineralogy and Petrology, v. 139, p. 684–703, https://doi.org/10.1007/s004100000172.

De Astis, G., Kempton, P.D., Peccerillo, A., and Wu, T.W., 2006, Trace element and isotopic variations from Mt. Vulture to Campanian volcanoes: Constraints for slab detachment and mantle inflow beneath southern Italy: Contributions to Mineralogy and Petrology, v. 151, p. 331–351, https://doi.org/10.1007/s00410-006-0062-y.

Del Moro, A., Gioncada, A., Pinarelli, L., Sbrana, A., and Joron, J.L., 1998, Sr, Nd, and Pb isotope evidence for open system evolution at Vulcano, Aeolian Arc, Italy: Lithos, v. 43, p. 81–106, https://doi.org/10.1016/S0024-4937(98)00008-5.

Di Renzo, V., Vito, M.A., Arienzo, I., Carandente, A., Civetta, L., D'Antonio, M., Giordano, F., Orsi, G., and Tonarini, S., 2007, Magmatic history of Somma-Vesuvius on the basis of new geochemical and isotopic data from a deep borehole (Camaldoli della Torre): Journal of Petrology, v. 48, p. 753–784, https://doi.org/10.1093/petrology/egl081.

Downes, H., Dupuy, C., and Leyreloup, A.F., 1990, Crustal evolution of the Hercynian belt of Western Europe: Evidence from lower-crustal granulitic xenoliths (French Massif Central): Chemical Geology, v. 83, p. 209–231, https://doi.org/10.1016/0009-2541(90)90281-B.

Downes, H., Kempton, P.D., Briot, D., Harmon, R.S., and Leyreloup, A.F., 1991, Pb and O systematics in granulite facies xenoliths, French Massif Central: Implications for crustal processes:

Earth and Planetary Science Letters, v. 102, p. 342–357, https://doi.org/10.1016/0012-821X(91)90028-G.
Downes, H., Shaw, A., Williamson, B.J., and Thirlwall, M.F., 1997, Sr, Nd and Pb isotopes of Hercynian granodiorites and monzogranites, Massif Central, France: Chemical Geology, v. 136, p. 99–122, https://doi.org/10.1016/S0009-2541(96)00141-6.
Downes, H., Thirlwall, M.F., and Trayhorn, S.C., 2001, Miocene subduction-related magmatism in Sardinia: Sr-Nd and oxygen isotopic evidence for mantle source enrichment: Journal of Volcanology and Geothermal Research, v. 106, p. 1–22, https://doi.org/10.1016/S0377-0273(00)00269-9.
Dufek, J., and Bergantz, G.W., 2005, Lower crustal magma genesis and preservation: A stochastic framework for the evaluation of basalt–crust interaction: Journal of Petrology, v. 46, no. 11, p. 2167–2195, https://doi.org/10.1093/petrology/egi049.
Fornaseri, M., Scherillo, A., and Ventriglia, U., 1963, La Regione Vulcanica dei Colli Albani: Consiglio Nazionale delle Ricerche, Rome, Italy, 561 p.
Francalanci, L., Taylor, S.R., McCulloch, M.T., and Woodhead, J.D., 1993, Geochemical and isotopic variations in the calc-alkaline rocks of Aeolian arc, southern Tyrrhenian Sea, Italy: Constraints on magma genesis: Contributions to Mineralogy and Petrology, v. 113, p. 300–313, https://doi.org/10.1007/BF00286923.
Franciosi, L., Lustrino, M., Melluso, L., Morra, V., and D'Antonio, M., 2003, Geochemical characteristics and mantle sources of the Oligo-Miocene primitive basalts from Sardinia: The role of subduction components: Ofioliti, v. 28, p. 105–114.
Freymuth, H., Brandmeier, M., and Wörner, G., 2015, The origin and crust/mantle mass balance of Central Andean ignimbrite magmatism constrained by oxygen and strontium isotopes and erupted volumes: Contributions to Mineralogy and Petrology, v. 169, no. 58, 24 p., https://doi.org/10.1007/s00410-015-1152-5.
Gao, P., Zheng, Y.-F., and Zhao, Z.-F., 2016, Experimental melts from crustal rocks: A lithochemical constraint on granite petrogenesis: Lithos, v. 266–267, p. 133–157, https://doi.org/10.1016/j.lithos.2016.10.005.
Gasperini, D., Blichert-Toft, J., Bosch, D., Del Moro, A., Macera, P., and Albarède, F., 2002, Upwelling of deep mantle material through a plate window: Evidence from the geochemistry of Italian basaltic volcanics: Journal of Geophysical Research: Solid Earth, v. 107, p. ECV 7-1–ECV 7-19, 2367, https://doi.org/10.1029/2001JB000418.
Gattacceca, J., Deino, A., Rizzo, R., Jones, D.S., Henry, B., Beaudoin, B., and Vadeboin, F., 2007, Miocene rotation of Sardinia: New paleomagnetic and geochronological constraints and geodynamic implications: Earth and Planetary Science Letters, v. 258, p. 359–377, https://doi.org/10.1016/j.epsl.2007.02.003.
Gioncada, A., Mazzuoli, R., Bisson, M., and Pareschi, M.T., 2003, Petrology of volcanic products younger than 42 ka on the Lipari-Vulcano complex (Aeolian Islands, Italy): An example of volcanism controlled by tectonics: Journal of Volcanology and Geothermal Research, v. 122, p. 191–220, https://doi.org/10.1016/S0377-0273(02)00502-4.
Gisbert, G., and Gimeno, D., 2017, Ignimbrite correlation using whole-rock geochemistry: An example from the Sulcis (SW Sardinia, Italy): Geological Magazine, v. 154, p. 740–756, https://doi.org/10.1017/S0016756816000327.
Grousset, F.E., Parra, M., Bory-à, A., Martinez, P., Bertrand, P., Shimmield, G., and Ellam, R., 1998, Saharan wind regimes traces by the Sr–Nd isotopic composition of subtropical sediments: Last glacial maximum vs today: Quaternary Science Reviews, v. 17, p. 395–409, https://doi.org/10.1016/S0277-3791(97)00048-6.
Guarino, V., Fedele, L., Franciosi, L., Lonis, R., Lustrino, M., Marrazzo, M., Melluso, L., Morra, V., Rocco, I., and Ronga, F., 2011, Mineral compositions and magmatic evolution of the calcalkaline rocks of northwestern Sardinia, Italy: Periodico di Mineralogia, v. 80, p. 517–545.
Gueguen, E., Doglioni, C., and Fernandez, M., 1998, On the post-25 Ma geodynamic evolution of the western Mediterranean: Tectonophysics, v. 298, p. 259–269, https://doi.org/10.1016/S0040-1951(98)00189-9.
Handley, H.K., Turner, S., Macpherson, C.G., Gertisser, R., and Davidson, J.P., 2011, Hf–Nd isotope and trace element constraints on subduction inputs at island arcs: Limitations of Hf anomalies as sediment input indicators: Earth and Planetary Science Letters, v. 304, p. 212–223, https://doi.org/10.1016/j.epsl.2011.01.034.
Hanyu, T., Tatsumi, Y., and Nakai, S., 2002, Contribution of slab-melts to the formation of high-Mg andesite magmas; Hf isotopic evidence from SW Japan: Geophysical Research Letters, v. 29, 2051, https://doi.org/10.1029/2002GL015856.
Hawkesworth, C.J., and Vollmer, R., 1979, Crustal contamination versus enriched mantle: $^{143}Nd/^{144}Nd$ and $^{87}Sr/^{86}Sr$ evidence from the Italian volcanics: Contributions to Mineralogy and Petrology, v. 69, p. 151–165, https://doi.org/10.1007/BF00371858.
Hickey-Vargas, R., Holbik, S., Tormey, D., Frey, F.A., and Moreno Roa, H., 2016, Basaltic rocks from the Andean Southern Volcanic Zone: Insights from the comparison of along-strike and small-scale geochemical variations and their sources: Lithos, v. 258–259, p. 115–132, https://doi.org/10.1016/j.lithos.2016.04.014.
Hidalgo, Sl., Gerbe, M.C., Martin, H., Samaniego, P., and Bourdon, E., 2012, Role of crustal and slab components in the Northern Volcanic Zone of the Andes (Ecuador) constrained by Sr–Nd–O isotopes: Lithos, v. 132–133, p. 180–192, https://doi.org/10.1016/j.lithos.2011.11.019.
Hildreth, W., and Moorbath, S., 1988, Crustal contributions to arc magmatism in the Andes of central Chile: Contributions to Mineralogy and Petrology, v. 98, p. 455–489, https://doi.org/10.1007/BF00372365.
Irvine, T.N., and Baragar, W.R.A., 1971, A guide to the chemical classification of the common volcanic rocks: Canadian Journal of Earth Sciences, v. 8, p. 523–548, https://doi.org/10.1139/e71-055.
Jicha, B.R., Singer, B.S., Brophy, J.G., Fournelle, J.H., Johnson, C.M., Beard, B.L., Lapen, T.J., and Mahlen, T.J., 2004, Variable impact of the subducted slab on Aleutian Island arc magma sources: Evidence from Sr, Nd, Pb, and Hf isotopes and trace element abundances: Journal of Petrology, v. 45, p. 1845–1875, https://doi.org/10.1093/petrology/egh036.
Johnson, M.C., and Plank, T., 1999, Dehydration and melting experiments constrain the fate of subducted sediments: Geochemistry, Geophysics, Geosystems, v. 1, no. 12, https://doi.org/10.1029/1999GC000014.
Kempton, P.D., 1987, Mineralogic and geochemical evidence for differing styles of metasomatism in spinel lherzolite xenoliths: Enriched mantle source regions of basalts? *in* Menzies, M., and Hawkesworth, C.J., eds., Mantle Metasomatism: London, UK, Academic Press, p. 45–89.
Kempton, P.D., 1995, Common Pb chemical procedures for silicate rocks and minerals, methods of data correction and an assessment of data quality at the NERC Isotope Geosciences Laboratory: NIGL Report Series, no. 78, 26 p.
Kempton, P.D., and Dungan, M.A., 1989, Geology and petrology of basalts and included mafic, ultramafic and granulitic xenoliths from the Geronimo volcanic field, southeastern Arizona, *in* Chapin, C.E., and Zidek, J., eds., Field Excursions to Volcanic Terranes in the Western United States, Volume I: Southern Rocky Mountain Region: Socorro, New Mexico, USA, New Mexico Bureau of Mines and Mineral Resources, v. 46, p. 161–173.
Kempton, P.D., Nowell, G.M., Fitton, J.G., Saunders, A.D., and Taylor, R.N., 2000, The Iceland plume in space and time: A Sr-Nd-Pb-Hf study of the North Atlantic rifted margin: Earth and Planetary Science Letters, v. 177, p. 255–271, https://doi.org/10.1016/S0012-821X(00)00047-9.
Kempton, P.D., Pearce, J.A., Gill, J., and Barry, T.L., 2001, Mantle domain boundaries in the Western Pacific: Evidence from Nd-Hf Isotope Systematics: Journal of Conference Abstracts, v. 6, p. 418.
Keppler, H., 2017, Fluids and trace element transport in subduction zones: The American Mineralogist, v. 102, p. 5–20, https://doi.org/10.2138/am-2017-5716.
Klaver, M., Djuly, T., de Graaf, S., Sakes, A., Wijbrans, J., Davies, G., and Vroon, P., 2015, Temporal and spatial variations in provenance of Eastern Mediterranean Sea sediments: Implications for Aegean and Aeolian arc volcanism: Geochimica et Cosmochimica Acta, v. 153, p. 149–168, https://doi.org/10.1016/j.gca.2015.01.007.
Kuno, H., 1968, Origin of andesite and its bearing on arc structure: Bulletin Volcanologique, v. 32, p. 141–176, https://doi.org/10.1007/BF02596589.
Kumar, A., Abouchami, W., Galer, S.J.G., Garrison, V.H., Williams, E., Garrison, V.H., Williams, E., and Andreae, M.O., 2014, A radiogenic isotope tracer study of transatlantic dust transport from Africa to the Caribbean: Atmospheric Environment, v. 82, p. 130–143, https://doi.org/10.1016/j.atmosenv.2013.10.021.
Lambart, S., Laporte, D., and Schiano, P., 2013, Markers of the pyroxenite contribution in the major-element compositions of oceanic basalts: Review of the experimental constraints: Lithos, v. 160–161, p. 14–36, https://doi.org/10.1016/j.lithos.2012.11.018.
Landi, P., Corsaro, R.A., Francalanci, L., Civetta, L., Miraglia, L., Pompilio, M., and Tesoro, R., 2009, Magma dynamics during the 2007 Stromboli eruption (Aeolian Islands, Italy): Mineralogical, geochemical and isotopic data: Journal of Volcanology and Geothermal Research, v. 182, p. 255–268, https://doi.org/10.1016/j.jvolgeores.2008.11.010.
Le Maitre, R.W., Streckeisen, A., Zanettin, B., Le Bas, M.J., Bonin, M., Bateman, P., Bellieni, G., Duděk, A., Efremova, S., Keller, J., Lameyre, J., Sabine, P.A., Schmid, R., Sørensen, H., and

Wolley, A.R., 2002, Igneous Rocks: A Classification and Glossary of Terms: Cambridge, UK, Cambridge University Press, 236 p.
Lecca, L., Lonis, R., Luxoro, S., Melis, F., Secchi, F., and Brotzu, P., 1997, Oligo-Miocene volcanic sequences and rifting stages in Sardinia: A review: Periodico di Mineralogia, v. 66, p. 7–61.
Lustrino, M., Morra, V., Fedele, L., and Serracino, M., 2007, The transition between 'orogenic' and 'anorogenic' magmatism in the western Mediterranean area: The Middle Miocene volcanic rocks of Isola del Toro (SW Sardinia, Italy): Terra Nova, v. 19, p. 148–159, https://doi.org/10.1111/j.1365-3121.2007.00730.x.
Lustrino, M., Morra, V., Fedele, L., and Franciosi, L., 2009, Beginning of the Apennine subduction system in central western Mediterranean: Constraints from Cenozoic "orogenic" magmatic activity of Sardinia, Italy: Tectonics, v. 28, TC5016, https://doi.org/10.1029/2008TC002419.
Lustrino, M., Duggen, S., and Rosenberg, C.L., 2011, The Central-Western Mediterranean: Anomalous igneous activity in an anomalous collisional tectonic setting: Earth-Science Reviews, v. 104, p. 1–40, https://doi.org/10.1016/j.earscirev.2010.08.002.
Lustrino, M., Fedele, L., Melluso, L., Morra, V., Ronga, F., Geldmacher, J., Duggen, S., Agostini, S., Cucciniello, C., Franciosi, L., and Meisel, T., 2013, Origin and evolution of Cenozoic magmatism of Sardinia (Italy): A combined isotopic (Sr–Nd–Pb–O–Hf–Os) and petrological view: Lithos, v. 180–181, p. 138–158, https://doi.org/10.1016/j.lithos.2013.08.022.
Lustrino, M., Fedele, L., Agostini, S., Di Vincenzo, G., and Morra, V., 2017, Eocene-Miocene igneous activity in Provence (SE France): $^{40}Ar/^{39}Ar$ data, geochemical-petrological constraints and geodynamic implications: Lithos, v. 288–289, p. 72–90, https://doi.org/10.1016/j.lithos.2017.07.008.
Mamani, M., Wörner, G., and Sempere, T., 2010, Geochemical variations in igneous rocks of the Central Andean orocline (13°S to 18°S): Tracing crustal thickening and magma generation through time and space: Geological Society of America Bulletin, v. 122, no. 1–2, p. 162–182, https://doi.org/10.1130/B26538.1.
Mattioli, M., Guerrera, F., Tramontana, M., Raffaelli, G., and D'Atri, M., 2000, High-Mg Tertiary basalts in Southern Sardinia (Italy): Earth and Planetary Science Letters, v. 179, p. 1–7, https://doi.org/10.1016/S0012-821X(00)00103-5.
Melekhova, E., Blundy, J., Robertson, R., and Humphreys, M.C.S., 2015, Experimental evidence for polybaric differentiation of primitive arc basalt beneath St. Vincent, Lesser Antilles: Journal of Petrology, v. 56, no. 1, p. 161–192, https://doi.org/10.1093/petrology/egu074.
Montigny, L., Edel, J.B., and Thuizat, R., 1981, Oligo-Mio rotation of Sardinia: K-Ar ages and paleomagnetic data of Tertiary volcanism: Earth and Planetary Science Letters, v. 54, p. 261–271, https://doi.org/10.1016/0012-821X(81)90009-1.
Morra, V., Secchi, F.A., and Assorgia, A., 1994, Petrogenetic significance of peralkaline rocks from Cenozoic calc-alkaline volcanism from Sardinia, Italy: Chemical Geology, v. 118, p. 109–142, https://doi.org/10.1016/0009-2541(94)90172-4.
Morra, V., Secchi, F.A.G., Melluso, L., and Franciosi, L., 1997, High-Mg subduction-related Tertiary basalts in Sardinia, Italy: Lithos, v. 40, p. 69–91, https://doi.org/10.1016/S0024-4937(96)00028-X.
Münker, C., Worner, G., Yogodzinski, G., and Churikova, T., 2004, Behaviour of high field strength elements in subduction zones: Constraints from Kamchatka-Aleutian arc lavas: Earth and Planetary Science Letters, v. 224, p. 275–293, https://doi.org/10.1016/j.epsl.2004.05.030.
Muroi, R., and Arai, S., 2014, Formation process of olivine and clinopyroxene cumulates inferred from Takashima xenoliths, southwest Japan arc: Journal of Mineralogical and Petrological Sciences, v. 109, p. 79–84, https://doi.org/10.2465/jmps.131003.
Orsi, G., Civetta, L., D'Antonio, M., Di Girolamo, P., and Piochi, M., 1995, Step-filling and development of a three-layer magma chamber: The Neapolitan Yellow Tuff case history: Journal of Volcanology and Geothermal Research, v. 67, p. 291–312, https://doi.org/10.1016/0377-0273(94)00119-2.
Pappalardo, L., Piochi, M., D'Antonio, M., Civetta, L., and Petrini, R., 2002, Evidence for multistage magmatic evolution during the past 60 kyr at Campi Flegrei (Italy) deduced from Sr, Nd and Pb isotope data: Journal of Petrology, v. 43, p. 1415–1434, https://doi.org/10.1093/petrology/43.8.1415.
Patchett, P.J., White, W.M., Feldmann, H., Kielinczuk, S., and Hofmann, A.W., 1984, Hafnium/rare earth element fractionation in the sedimentary system and crustal recycling into the Earth's mantle: Earth and Planetary Science Letters, v. 69, p. 365–378, https://doi.org/10.1016/0012-821X(84)90195-X.
Peacock, M.A., 1931, Classification of igneous rock series: The Journal of Geology, v. 39, p. 54–67, https://doi.org/10.1086/623788.
Pearce, J.A., Baker, P.E., Harvey, P.E., and Luff, I.W., 1995, Geochemical evidence for subduction fluxes, mantle melting and fractional crystallization beneath the South Sandwich Island Arc: Journal of Petrology, v. 36, p. 1073–1109, https://doi.org/10.1093/petrology/36.4.1073.
Pearce, J.A., Kempton, P.D., and Gill, J.B., 2007, Hf-Nd evidence for the origin and distribution of mantle domains in the SW Pacific: Earth and Planetary Science Letters, v. 260, p. 98–114, https://doi.org/10.1016/j.epsl.2007.05.023.
Peccerillo, A., and Lustrino, M., 2005, Compositional variations of the Plio-Quaternary magmatism in the circum-Tyrrhenian area: Deep versus shallow mantle processes, *in* Foulger, G.R., Natland, J.H., Presnall, D.C., and Anderson, D.L., eds., Plates, Plumes and Paradigms: Geological Society of America Special Paper 388, p. 421–434, https://doi.org/10.1130/0-8137-2388-4.421.
Peccerillo, A., Kempton, P.D., Harmon, R.S., Wu, T.W., Santo, A.P., Boyce, A.J., and Tripodo, A., 1993, Petrological and geochemical characteristics of the Alicudi Volcano, Aeolian Islands, Italy: Implications for magma genesis and evolution: Acta Vulcanologica, v. 3, p. 235–249.
Peccerillo, A., Dallai, L., Frezzotti, M.L., and Kempton, P.D., 2004, Sr-Nd-Pb-O isotopic evidence for decreasing crustal contamination with ongoing magma evolution at Alicudi Volcano (Aeolian Arc, Italy): Implications for style of magma-crust interaction and for mantle source compositions: Lithos, v. 78, p. 217–233, https://doi.org/10.1016/j.lithos.2004.04.040.
Perinelli, C., Gaeta, M., and Armienti, P., 2017, Cumulate xenoliths from Mt. Overlord, northern Victoria Land, Antarctica: A window into high pressure storage and differentiation of mantle-derived basalts: Lithos, v. 268–271, p. 225–239, https://doi.org/10.1016/j.lithos.2016.10.027.
Perini, G., Francalanci, L., Davidson, J.P., and Conticelli, S., 2004, The petrogenesis of Vico Volcano, Central Italy: An example of low scale mantle heterogeneity: Journal of Petrology, v. 45, p. 139–182, https://doi.org/10.1093/petrology/egg084.
Pourmand, A., Prospero, J.M., and Sharifi, A., 2014, Geochemical fingerprinting of trans-Atlantic African dust based on radiogenic Sr-Nd-Hf isotopes and rare earth element anomalies: Geology, v. 42, no. 8, p. 675–678, https://doi.org/10.1130/G35624.1.
Prelević, D., Stracke, A., Foley, S.F., Romer, R.L., and Conticelli, S., 2010, Hf isotope compositions of Mediterranean lamproites: Mixing of melts from asthenosphere and crustally contaminated mantle lithosphere: Lithos, v. 119, p. 297–312, https://doi.org/10.1016/j.lithos.2010.07.007.
Réhault, J.-P., Boillet, G., and Mauffret, A., 1984, The Western Mediterranean basin geological evolution: Marine Geology, v. 55, p. 447–477, https://doi.org/10.1016/0025-3227(84)90081-1.
Réhault, J.-P., Honthaas, C., Guennoc, P., Bellon, H., Ruffer, G., Cotton, J., Sosson, M., and Maury, R.C., 2012, Offshore Oligo-Miocene volcanic fields within the Corsica-Liguria Basin: Magmatic diversity and slab evolution in the western Mediterranean Sea: Journal of Geodynamics, v. 58, p. 73–95, https://doi.org/10.1016/j.jog.2012.02.003.
Rogers, N.W., Hawkesworth, C.J., Parker, R.J., and Marsh, J.S., 1985, The geochemistry of potassic lavas from Vulsini, Central Italy, and implications for the mantle enrichment processes beneath the Roman Province: Contributions to Mineralogy and Petrology, v. 90, p. 244–257, https://doi.org/10.1007/BF00378265.
Rosenbaum, G., Lister, G.S., and Duboz, C., 2002, Reconstruction of the tectonic evolution of the western Mediterranean since the Oligocene, *in* Rosenbaum, G., and Lister, G.S., eds., Reconstruction of the Evolution of the Alpine-Himalayan Orogen: Journal of the Virtual Explorer, v. 8, p 107–130, https://doi.org/10.3809/jvirtex.vol.2002.008.
Rossi, Ph., Oggiano, G., and Cocherie, A., 2009, A restored section of the "Southern Variscan realm" across the Corsica-Sardinia microcontinent: Comptes Rendus Geoscience, v. 341, p. 224–238, https://doi.org/10.1016/j.crte.2008.12.005.
Santo, A.P., Jacobsen, S.B., and Baker, J., 2004, Evolution and genesis of calc-alkaline magmas at Filicudi volcano, Aeolian Arc (Southern Tyrrhenian Sea, Italy): Lithos, v. 72, p. 73–96, https://doi.org/10.1016/j.lithos.2003.08.005.
Scheuvens, D., Schütz, L., Kandler, K., Ebert, M., and Weinbruch, S., 2013, Bulk composition of northern African dust and its source sediments—A compilation: Earth-Science Reviews, v. 116, p. 170–194, https://doi.org/10.1016/j.earscirev.2012.08.005.
Solano, J.M.S., Jackson, M.D., Sparks, R.S.J., Blundy, J.D., and Annen, C., 2012, Melt segregation in deep crustal hot zones: Mechanism for chemical differentiation, crustal assimilation and the formation of evolved magmas: Journal of Petrology, v. 53, p. 1999–2026, https://doi.org/10.1093/petrology/egs041.
Spence, E.A., 2012, Using isotopes to identify upper mantle sources of prehistoric magmatism on Mount Etna and its relation to regional volcanism [M Res. thesis]: Birkbeck, UK, University College London, 87 p.

Splendore, R., and Marotta, A.M., 2013, Crust-mantle mechanical structure in the Central Mediterranean region: Tectonophysics, v. 603, p. 89–103, https://doi.org/10.1016/j.tecto.2013.05.017.

Stracke, A., 2012, Earth's heterogeneous mantle: A product of convection-driven interaction between crust and mantle: Chemical Geology, v. 330–331, p. 274–299, https://doi.org/10.1016/j.chemgeo.2012.08.007.

Todt, W., Cliff, R.A., Hanser, A., and Hofmann, A.W., 1996, Evaluation of a ^{202}Pb–^{205}Pb double spike for high-precision lead isotope analysis, *in* Basu, A., and Hart, S., eds., Earth Processes: Reading the Isotopic Code: Washington, D.C., USA, American Geophysical Union, https://doi.org/10.1029/GM095p0429.

Tollstrup, D., and Gill, J., 2005, Hafnium systematics of the Mariana arc: Evidence for sediment melt and residual phases: Geology, v. 33, p. 737–740, https://doi.org/10.1130/G21639.1.

Tollstrup, D., Gill, J., Kent, A., Prinkey, D., Williams, R., Tamura, Y., and Ishizuka, O., 2010, Across-arc geochemical trends in the Izu-Bonin arc: Contributions from subducted slab, revisited: Geochemistry, Geophysics, Geosystems, v. 11, no. 1, p. 1525–2027, https://doi.org/10.1029/2009GC002847.

Tommasini, S., Poli, G., and Halliday, A.N., 1995, The role of sediment subduction and crustal growth in Hercynian plutonism: Isotopic and trace element evidence from the Sardinia-Corsica batholiths: Journal of Petrology, v. 36, p. 1305–1332, https://doi.org/10.1093/petrology/36.5.1305.

Tonarini, S., Armienti, P., D'Orazio, M., Innocenti, F., Pompilio, M., and Petrini, R., 1995, Geochemical and isotopic monitoring of Mt. Etna 1989–1993 eruptive activity: Bearing on the shallow feeding system: Journal of Volcanology and Geothermal Research, v. 64, p. 95–115, https://doi.org/10.1016/0377-0273(94)00039-J.

Tonarini, S., D'Orazio, M., Armienti, P., Innocenti, F., and Scribano, V., 1996, Geochemical features of eastern Sicily lithosphere as probed by Hyblean xenoliths and lavas: European Journal of Mineralogy, v. 8, p. 1153–1174, https://doi.org/10.1127/ejm/8/5/1153.

Toothill, J., Williams, C.A., Macdonald, R., Turner, S.P., Rogers, N.W., Hawkesworth, C.J., Jerram, D.A., Ottley, C.J., and Tindle, A.G., 2007, A complex petrogenesis for an arc magmatic suite, St Kitts, Lesser Antilles: Journal of Petrology, v. 48, p. 3–42, https://doi.org/10.1093/petrology/egl052.

Trua, T., Esperança, S., and Mazzuoli, R., 1998, The evolution of the lithospheric mantle along the N. African Plate: Geochemical and isotopic evidence from the tholeiitic and alkaline volcanic rocks of the Hyblean plateau, Italy: Contributions to Mineralogy and Petrology, v. 131, p. 307–322, https://doi.org/10.1007/s004100050395.

Trua, T., Serri, G., and Marani, M.P., 2003, Lateral flow of African mantle below the nearby Tyrrhenian plate: Geochemical evidence: Terra Nova, v. 15, p. 433–440, https://doi.org/10.1046/j.1365-3121.2003.00509.x.

Vervoort, J.D., Patchett, P.J., Albarède, F., Blichert-Toft, J., Rudnick, R., and Downes, H., 2000, Hf-Nd isotopic evolution of the lower crust: Earth and Planetary Science Letters, v. 181, p. 115–129, https://doi.org/10.1016/S0012-821X(00)00170-9.

Vervoort, J.D., Plank, T., and Prytulak, J., 2011, The Hf–Nd isotopic composition of marine sediments: Geochimica et Cosmochimica Acta, v. 75, p. 5903–5926, https://doi.org/10.1016/j.gca.2011.07.046.

Viccaro, M., and Cristofolini, R., 2008, Nature of mantle heterogeneity and its role in the short-term geochemical and volcanological evolution of Mt. Etna (Italy): Lithos, v. 105, p. 272–288, https://doi.org/10.1016/j.lithos.2008.05.001.

Viccaro, M., Nicotra, E., Millar, I.L., and Cristofolini, R., 2011, The magma source at Mount Etna volcano: Perspectives from the Hf isotope composition of historic and recent lavas: Chemical Geology, v. 281, p. 343–351, https://doi.org/10.1016/j.chemgeo.2010.12.020.

Woodhead, J.D., Hergt, J.M., Davidson, J.P., and Eggins, S.M., 2001, Hafnium isotope evidence for 'conservative' element mobility during subduction zone processes: Earth and Planetary Science Letters, v. 192, p. 331–346, https://doi.org/10.1016/S0012-821X(01)00453-8.

Zamboni, D., Gazel, E., Ryan, J., Cannatelli, C., Lucchi, F., Atlas, Z., Trela, J., Mozza, S., and DeVivo, B., 2016, Contrasting sediment melt and fluid signatures for magma components in the Aeolian Arc: Implications for numerical modeling of subduction zones: Geochemistry, Geophysics, Geosystems, v. 17, p. 2034–2053, https://doi.org/10.1002/2016GC006301.

Zirakparvar, N.A., 2017, Constraints on Lu-Hf and Nb-Ta systematics in globally subducted oceanic crust from a survey of orogenic eclogites and amphibolites: Geochemistry, Geophysics, Geosystems, v. 17, p. 1540–1557, https://doi.org/10.1002/2016GC006377.